

Response to reviewer comments.

We would like to thank all reviewers for their effort to provide a constructive review and suggestions to improve the manuscript. We considered each comment and included most of the suggested changes. In those cases where changes were not made, we explained why we disagree or the changes are not possible to add. Our replies can be found below each comment.

For an overview; the main changes comprise:

- Added a short, general description of oceanographic aspects relevant for the study
- Added estimation of advective transport
- Added more information for sea-air flux estimation
- Added description of current speed during sampling campaigns using modelled forecasts, the data is shown in Supplementary Material 2 and 3
- Added data of reference station in Supplementary Material 4
- Revised the averaging of the constant k' and added a discussion why no methanotrophs were detected with the molecular methods used
- Estimated critical parameter D_V of model according to the equation by Osborn (1980) relating the dissipation rate of turbulent kinetic energy with the buoyancy frequency
- Added a sensitivity test of the model to the discussion of model results
- Added comments why methanotrophy remained low even methane was sufficiently available
- Changed some references

Interactive comment on “Seasonal methane accumulation and release from a gas emission site in the central North Sea” by S. Mau et al.

Anonymous Referee #1

Received and published: 2 January 2015

Mau et al “Seasonal methane accumulation and release from a gas emission site in the central North Sea” (manuscript # bg-2014-506), provides a welcome analysis of the dynamics of methane flux in a seepage-influenced coastal shelf site. This analysis includes summer and winter measurements of methane concentrations and oxidation rates, in the context of thermal stratification and horizontal and vertical transport processes. The data and analysis contributes nicely to modeling the contribution of coastal marine sources to global methane inventories. General comments: The analysis was well-supported across various metrics. Incorporation of new data into the existing literature was also generally good, and the data fit well with past estimates of methane flux. The main conclusions are sound. I have several questions for the authors.

Specific comments:

First, is it possible to determine if in situ methane production is occurring and biasing rate measurements? See e.g. Tang et al 2014, Limnology and Oceanography. This and other sources suggest that methane production in relatively shallow oxygenated waters can occur – possibly arising from methanogenic organisms tightly coupled to photosynthesizers. Methane production and consumption may be likewise tightly coupled between microorganisms, and tracers may not compete well as a substrate in such a scenario (Furthermore – particularly when considering a low ‘on rate’/‘enzymatic uptake’ as speculated in this paper, the added mass of heavy isotopes may introduce significant bias in rate estimates).

Author: In situ methane production is difficult to obtain due to the lack of knowledge, how methane is generated in oxic waters. One can determine the increase in methane concentration or use ^{14}C -bicarbonate or ^{14}C -acetate as it is done in sediments, but in the water column also dimethylsulfoniopropionate (DMSP) (Damm et al., 2010) or methylphosphonic acid (MPn) (Karl et al., 2008; Metcalf et al., 2012) have been reported as possible substrates. However, in the study area methane production is most likely much smaller than methane originating from bubble dissolution. For comparison, we measured a concentration of 20 nM (maximum was 25 nM) at a reference site, 32 km away, with an oxidation rate of 0.19 nM d⁻¹. Even if one

assumes methane production/consumption to be tightly coupled, these organisms appear not to be able to consume additional methane.

Indeed, biological uptake tends to prefer light isotopes and a bias is most likely. However, the bias due to heavy isotopes is not known. Considering that a common isotopic effect is given in per mill and that duplicates differ by up to 30%, the isotopic bias might be arguable significant.

Second, the Michaelis Menten averaging may not be appropriate or valid. In Baani et al, two isoforms of pMMO are shown to have different kinetics of methane oxidation. On an environmental scale one expects widely disparate K_m 's from different isoforms, or homologs, of the same enzyme. Indeed, from a biochemical view, determination of K_m is most appropriate from purified enzymes - and not necessarily reliably determined otherwise, yes? Is it possible to provide an indication of error in your averaged K_m ? Or, perhaps bin the pre-averaged K_m measurements according to methane concentration to generate confidence levels that you are not averaging across different biochemical processes. There is more scatter in Figure 7 than I would have expected from the text.

Author: The range of possible K_m is shown in Fig. 7A. These K_m 's are not related to the data. And yes, K_m determined from an environmental sample is always a mixed K_m of different enzymes and different quantities of different enzymes. We did not average any K_m , we fitted a v_{max} and K_m to our data (CH_4 -concentration and MOx) according to eq. 6 (excluding the 7 data points with $MOx > 20 \text{ nM d}^{-1}$). The fitted curve has a R^2 of 0.81; we added this value to the text. Using methane concentrations from 1 to 500 nM and calculating the MOx taking eq.6 with the fitted parameters v_{max} and K_m , we can calculate k' , which is MOx divided by $[CH_4]$. Therefore, we use the equation and fitted parameters to derive a k' , which is based on 120 data points. If this method is used with other data of other regions, it might provide an understanding of the difference of v_{max} and K_m in environmental samples. Please note, that we revised this statement according to our response no. 5 to reviewer 3 (Page 15, Line 518-519). The scatter in the figure appears more significant than described in the text, because a lot of low rate and concentration measurements plot onto each other while higher rates and concentrations do not, but have been less often measured.

Lastly, it is not clear if you are posing that there is, or isn't, a microbial methane oxidizing community. What seems likely is that microbial methanotrophs are present in such low numbers and/or are such poor matches to your PCR primers that they are below detection. The latter of these possibilities has been directly demonstrated for marine planktonic methanotrophs (Hansman, 2008). Additional research using not only PCR but also methods with intrinsically less bias (e.g. SIP, metatranscriptomics) has demonstrated global cosmopolitan presence of canonical as well as unusual methanotrophs in bottom waters. These published findings pertain directly to the problem of primer bias in PCR (e.g. Li et al 2014, Env. Micr.) Shallower marine waters (<200m) in the Pacific, Atlantic, and the Gulf of Mexico are almost invariably devoid of detectable canonical methanotrophs - but can host unusual pmo variants including those from unusual phylogenies. Your results from a relatively shallow marine source relate directly to these published trends (e.g. Tavormina 2013 and references therein).

Author: We appreciate this constructive comment and added a few sentences stating your suggested possibility that known methanotrophs were not detected due to low number or inappropriate PCR primers. By using the common primer sets for the pmoA gene analysis, we did not obtain a positive PCR product, but we know that this does not mean that methanotrophs were absent. Other methods might be able to discover methanotrophs that did not match the used PCR-primers. We also stated that our finding is in accordance to others in shallow marine waters (Page 16, Line 534-540).

Technical comments:

Twice the word 'ascend' should more properly be 'ascent,' on page 18006 line 9 and page 18019 line 12 (Please also remove the comma following 'vent sites' on line 12).

Page 18009 line 16: The word 'gaschromatograph' is two words in the English language.

Page 18018, line 13: Please change 'but showed also' to 'but also showed' to correct the grammar.

Author: All these suggested corrections are done.

Can you provide some interpretation of these results? Do you believe that so few bands were clearly resolved because the original product was phylogenetically diverse, or was the quality of the original product poor? I would be curious to see the non-denaturing gel, to have a sense of the efficiency of the initial amplification reaction.

Author: We think that our DGGE-results are reliable, because we filtered 8 l of water, had good DNA-extracts, and used sufficient DNA for PCR. The quality of the winter samples was not as good as the quality

of the summer samples, but from our experience with pelagic samples, the results are plausible, too (Page 6, Line 209).

Page 18019 line 25 through page 18020 line 5: It may be appropriate to add Narvenkar et al 2013 to these references.

Author: The reference is included.

Page 18027 line 20: The Kessler estimates, which are environmentally based from a marine system, are more relevant than estimates from terrestrial organisms grown in culture. It may be appropriate to mention that few if any planktonic marine methanotrophs are currently available in culture thus doubling times are challenging to estimate.

Author: The suggested statement is included (Page 20, Line 686-687).

Table 2. Crespo-Medina (Nature Geoscience 2014) recently reported Mox rates surpassing those included in this table. Consider inclusion.

Author: The reference is included to complement the table.

Interactive comment on “Seasonal methane accumulation and release from a gas emission site in the central North Sea” by S. Mau et al.

Anonymous Referee #2

Received and published: 11 January 2015

the paper aims to constrain the seasonal variation of sea-air methane fluxes originating from shallow gas seepage, which is an important research question. The area of interest is located in a summerly thermally stratified part of the North Sea showing complete mixing in winter. A two layer model is introduced to investigate the seasonal changes of physical methane fluxes and relate those to microbial uptake.

The paper tackles complex tracer oceanographic problems requiring well planned sampling strategies, current measurements, solution of advection-diffusion equations and estimates about seasonal variation of vertical eddy diffusive transport. But the paper only presents an extremely simplified model. The oceanographic understanding appears limited and the model suffers from incompleteness and severe misunderstanding.

Author: The model is only part of the reported work and thought to support our conclusions, which were based on our data. It is not intended to be and nowhere near a detailed oceanographic model, which would need a more comprehensive data base. Our simple model is rather thought to check if our hypothesis to explain our data is correct. Biogeochemical measurements in summer and winter time in a shallow shelf sea area

indicate that a seasonal thermocline leads to an enrichment of methane below the thermocline. The winter data, which is currently rare and worthwhile to be published, shows that without a thermocline, there is no enrichment of methane. Furthermore, we discuss that microbial methane oxidation appears to be a small sink of methane. These findings hints to the conclusion, that most of the methane, which piles up below the seasonal thermocline, must be vented to the atmosphere as soon as the thermocline breaks down. We used the model to check if that hypothesis is plausible. Certainly more data collected at different times of the year and revised models are needed to further validate this hypothesis.

(1) The vertical eddy diffusivity k_z was estimated constant to $10e-4$ from literature (and tested for model uncertainty with $10-3$, and $10-5$ respectively). A seasonal built-up and destruction of a thermocline gives rise to a non-static k_z with variation by orders of magnitude throughout the year. The authors should have derived monthly k_z , e.g. by Thorpe Scale analyses, from CTD data.

Author: First of all, we used only one value of k_z (D_v in the text) for cross pycnocline mixing in the months from May until August, when there are two different water layers. The rest of the year, the water column is well mixed and there is only one water layer. Unfortunately, we do not have sufficient CTD data to be able to calculate representative k_z s. The data for the months May and June originate from an area within 3 to 6° E and 54 to 56° N as described in the manuscript, but were located closer to the coast than our study area. We lack any CTD-data of August. All CTD-data originate from water sampling and were not taken to investigate the turbulent diffusivity, thus we do not have sufficient replicates for a representative estimation of k_z . However, based on the constructive suggestion of the reviewer, we estimated k_z by using published dissipation rates of turbulent kinetic energy (Palmer et al., 2008, Thorpe et al., 2008) and calculating the buoyancy frequency from the available CTD-profiles. These results indicate that k_z is in the order of 10^{-4} to $10^{-6} \text{ m}^2 \text{ s}^{-1}$. Therefore, the value of k_z used for the model was appropriately chosen. We included this estimation in the manuscript (Page 18-19, Line 626-637).

(2) A 1D model is suggested to describe the flux of methane from the “deep” layer to the upper/mixed layer using Ficks 1st law. The authors derive model parameter dC_{CH_4}/dz from their field data by assuming a 1D case. This would require a distinct dC_{CH_4}/dz gradient with more or less homogeneous horizontal distribution of methane. However, the near field water column methane distribution pattern surrounding individual gas seepage clusters appears highly variable, i.e. with significant variation in three dimensions as shown by the authors themselves (Fig. 4). Surface methane values measured up to 2127nM with UWMS were reported. Obvious reasons are gas bubbles as visualized with acoustics. But the model assumes the only CH_4 source is the lowermost layer in their model. In summer the thermocline may reach down by 30m leaving a lowermost layer with 10m thickness. Methane gas bubbles easily bypass a $10\text{-}20\text{m}$ bottom layer without losing major fractions of their initial moles as shown in the cited paper McGinnis et al. (2006). No field data is provided about the crucial model parameters initial gas bubble size and methane mole fraction. Overall, bubbles most likely provide a strong source for methane input to the upper layer, but this is totally neglected in the model.

Author: 1D models are also used for modeling transport and reactions in marine sediments where methane and other chemical compounds also considerably vary over space. Similarly, bubble dissolution models do not take horizontal advection into account. These models (Leifer and Patro, 2002, McGinnis et al., 2006) suggest highest dissolution close to the sediment surface with an exponential decline towards shallower depth, thus, the main methane contribution occurs in the bottom layer, which is coherent with our data. Indeed part of the bubble dissolution takes place also in the upper layer, but if we assume that bubble dissolution is not affected by stratification as shown by Schneider von Deimling et al. (2011) at the Tommeliten site in the North Sea, then the source term for the upper layer would

always be the same. Therefore, the model values that are presented are conservative estimates and the model results are qualitatively correct. Gas bubble size and methane mole fraction were not measured during the two field campaigns as our intention was to investigate the seasonal variable methane distribution.

(3) monthly mean wind speed was taken for sea-air flux modeling. But the sea-air gas transfer is highly non-linear with wind speed and a monthly mean approach needs discussion. The sea-air flux potential is also governed by an interplay between strength and continuation of wind in relation to the remaining dissolved methane pool in the “wind-exhausted” layer. I.e. strong wind will not necessarily drive enhanced sea-air flux once the upper CH₄ layer was exhausted already.

Author: The formation and erosion of the seasonal thermocline forming a kind of barrier for dissolved methane was the objective of the model, thus, we used months as appropriate time period. Furthermore, monthly values of wind speed were readily accessible. However, based on this comment, we conducted a sensitivity check varying the parameters by +/- 10%. The sensitivity analysis showed that wind speed is the most sensitive parameter inducing a change of ~25% whereas surface water temperatures only yielded a difference by 1.5%. We added the sensitivity check to the discussion (Page 19, Line 659-663).

(4) The box model approach is only feasible in a closed system, but most likely the sampled area is an open system with significant advection and methane loss in various directions, and gas bubble methane dissolution up to the sea surface. The paper refers to using the disputable approach from Mau et al. (2012).

Author: We used a 1D model that indeed ignores any horizontal movement of methane. This very simple approach was used to test our understanding of the system. If horizontal effects would be taken into account, then the source term would need to be increased. The added quantity of methane would be horizontally advected and dispersed, but the vertical exchange processes would remain the same, thus, the outcome of the model is qualitatively correct. If we move horizontally away from our modelled source, then all concentrations would be lower due to horizontal eddy diffusion. Therefore, the limitation due to the thermocline would diminish with distance to the source and the sea-air flux would decrease. As we did not extrapolate over an area, but focused on the emission site, we argue that the model is sufficient for identifying a hypothetical seasonal cycle. More importantly, as the results fit to our observations, we think that the model is a valid approach.

(5) No current data are presented for the study site. But the North Sea is highly affected by the tides and the dominating M2 tide will likely cause significant current changes in amplitude and phase on an hourly timescale. Therefore the tempo-spatial methane distribution and the respective sampling are highly controlled by the actual current around the seep sites. The methane distribution pattern in winter shown in Fig. 4b is interpreted as a result from enhanced mixing. However, it could also be caused from current amplitude and direction “flushing” the seepage area with background water during the time of measurement (e.g. frontal jets have been discussed for the Dogger Bank with currents exceeding 15 cm s⁻¹, but are not mentioned in the paper).

Author: We agree that currents affect methane distribution, however, currents transport the methane, but do not decrease the concentration as no concentration gradient is included in the equation of the advective flux. We drew a sketch to show the influence of advection/currents (Fig. 1) showing that independent of the current velocity, the vertical concentration profile would always look similar: the concentration would exponentially decrease with distance to the seafloor. In addition, the seasonal thermocline will always limit vertical transport, thus, the model is qualitatively correct, but not necessarily quantitatively.

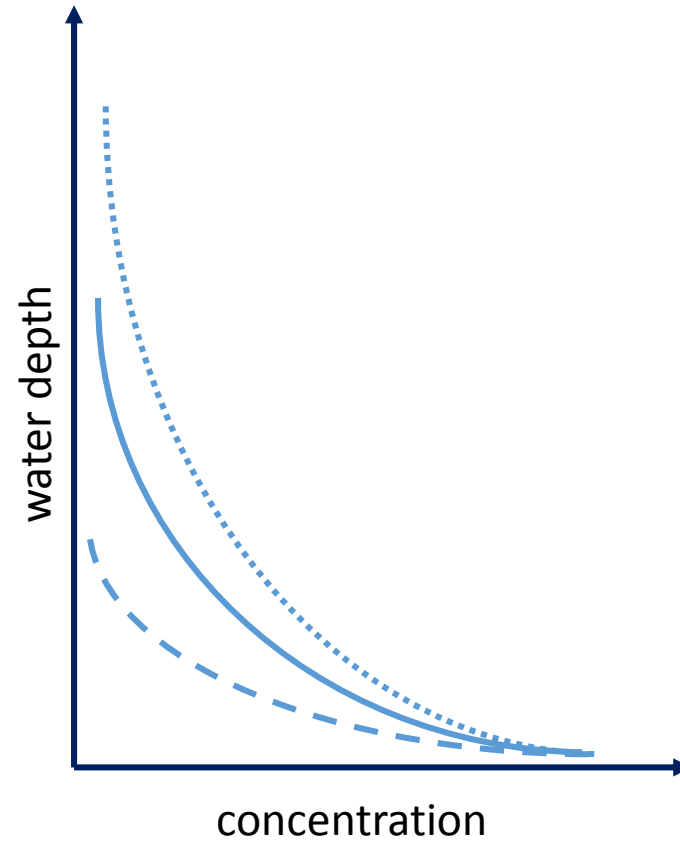
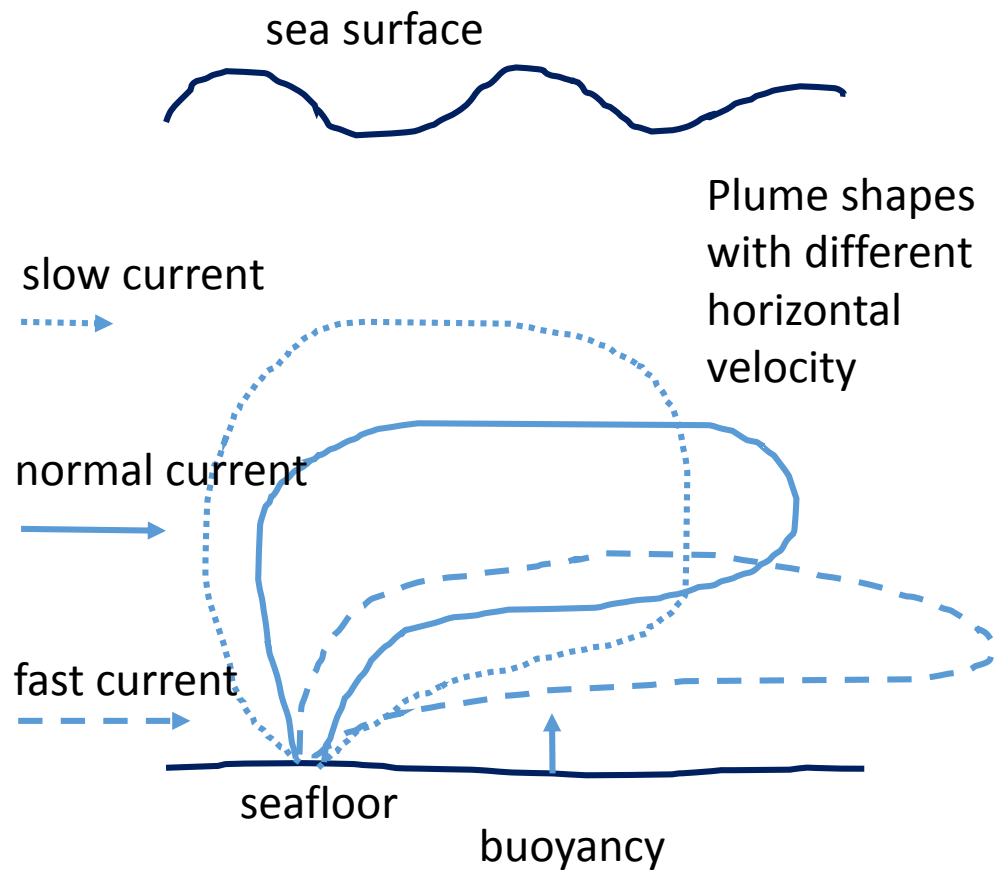


Fig. 1: Sketch of a methane plume with a constant source and buoyancy, but different water velocities. The shape of the vertical methane concentration profile would not change.

However, we included a description and added a plot to the supplementary material showing the east-west and north-south velocities of the currents during the sampling campaigns (Page 10-11, Line 348-355). The current data are modelled data by the BSH using wind and air temperature forecasts, thus, might be deficient. These data indicate that current direction was for most CTD stations to the north-west. Also the velocities were similar ranging between 0.1 and 0.2 m s⁻¹ during sampling campaigns. The lower concentrations in winter (i.e., western part of transect) were measured when the currents were less intense than the currents during sampling the eastern part of the transect, where higher concentrations were measured. Therefore, there was most likely no flushing.

No background CTD is available, and the amount of lateral input of methane into the layers remains unknown.

Author: Methane concentrations measured at a reference station were mentioned and we provide the data of the background CTD sampled 32 km away from the central station in summer (Page 11, Line 368-369). Methane concentrations at the reference station ranged between 17-25 nM and agree well with the ones published by Grundwald et al. (2009) for the German Bight.

The observation of enhanced MOx activity at depth is a valid observation. Also the high resolution in situ mass spectrometer CH₄ data in the near-field of gas seepage is valuable, because such data are very rare (but the respective 3D methane distribution it is not presented in the paper). The authors could think about a complete new story using such data. With the severe shortcomings of the model and missing current information the content of the paper can not support the conclusions. Therefore this paper can not be suggested for publication.

Author: We think that our conclusions are justified. Our main conclusion is that dissolved methane accumulates below the seasonal thermocline in summer and does not accumulate in winter when there is no stratification. Furthermore, detailed analysis of the methane oxidation measurements illustrate that methane oxidation is insufficient to significantly reduce the methane load. In combination, this suggests that the accumulated methane is at some time transferred to the atmosphere. Therefore, the conclusions are drawn from our measured data and, in addition, are supported by the model, which we argue to be qualitatively valid. Our conclusions and measurements fit to and extend the current knowledge of the sinks of methane emitted from shallow seep sites. We provide analysis in winter time and methane oxidation measurements, which are both rare data and reinforce the hypothesis of a higher methane release from the sea to the atmosphere in fall as reported by Glzew et al., 2013 for the Baltic Sea.

Technical Comments - equations are missing to allow for reconstructing the individual model steps

Author: On page 18014 line 12 we describe that eq. 3 and 4 are used in the model.

- Fig. 1: the wind recording station can hardly be detected. The flow pattern of the North Sea currents are provided, but the ones prevailing in the study area remain unclear, also in the text!

Author: We changed the color of the wind recording station for better visibility and included a description of the general oceanography and available modelled currents during the samplings campaigns (Page 4, Line 106-115; Page 10-11, Line 348-355).

- Fig. 2: poor quality and unclear. The three figures/inserts have three different color codes for the depth, confusing: : :. The UWMS sampling path could be better presented in 3D together with the methane concentration distribution in the results chapter.

Author: We changed the color code of the UWMS sampling path matching it to the flare imaging color scale, the other depth scale refers to the smooth topography. If we would have a scale for all, then the topography cannot be illustrated (would be one color). We think the discrete measured water samples and the UWMS-data are best compared as we illustrated it.

- Fig. 3: The CH₄ concentration profiles should be included here.

Author: The different methane concentration profiles are not as similar as e.g. the different temperature or salinity profiles, thus, we presented the data as contour plots to show more details.

- Sea-air flux calculations: rather provide classical and comprehensive work introducing the generic sea-air flux equation equ. 4 than self-citation.

Author: The citations were deleted.

Interactive comment on “Seasonal methane accumulation and release from a gas emission site in the central North Sea” by S. Mau et al.

Anonymous Referee #3

Received and published: 5 February 2015

The manuscript of Mau and co-authors describes the distribution of methane at a methane seep in the North Sea, together with the microbiological methane consuming process, its oxidation. The authors provide data from classical water sampling and additional in situ measurements of the methane concentration. Methane oxidation rates were measured with ³H-tracer, as an appropriate method. Thus, altogether a valuable data set. However, I have difficulties with the modelling part and the kinetics of the Mox rates of the manuscript. I therefore suggest "major revision".

Modelling 1) Based on the in situ data of methane, the authors have a 3-dimensional data set at hand. Thus it is not clear, why they restrict these data to simple box plots and further restricts the modelling to a 2-dimensional model. At the study site a 3-dimensional model with transport processes in all (or at least 4) directions would be more appropriate.

Author reply 1: We show 2D methane concentration data that are concentration profiles throughout the water column taken along a 6 km transect. We also show in situ UWMS-measurements that were collected near an active seep site in a very small area of 125 m by 150 m (Fig. 2). Therefore, the transect data show a much larger scale than the UWMS-data. The UWMS-data were included to prove that methane concentrations are similarly distributed over the tidal cycle in summer. For comparison of the two data sets (discrete sampling by CTD/rosette and UWMS-records), we found that a contour plot of the discrete samples and a box plot of the UWMS-records are most illustrative.

The model was used to correlate summer and winter methane concentrations and methane oxidation rates collected along the transect. The model is restricted to 1 dimension, the vertical dimension or height of the water column, which is (1) defined by the direction of the sea-air flux, which is one of the major sinks of dissolved methane in the water column. Furthermore (2), the main difference between

summer and winter data was the seasonal thermocline, which limits the vertical transport also in the dimension of the water column height. As we mentioned in the response to the second reviewer, if horizontal effects would be taken into account (3D), then the source term would need to be increased. The added quantity of methane would be horizontally advected and dispersed, but the vertical exchange processes would remain the same. Moreover, we would have been forced to include additional parameters such as the horizontal eddy diffusivity that all add uncertainty to the outcome of the model.

2) The transport processes used for the modelling are not clear to me. The authors neglect the advective process, as "currents only transport the water from the methane seep away". However, by doing so, at the study site the methane concentrations will decrease as methane rich water from the seep will be displaced / mixed with methane poor water. Thus, I think that dilution / mixing of water bodies through currents is an important factor, which should not be neglected.

Author reply 2: The same issue was raised by the second reviewer. We include our response to the other reviewer here again: We agree that currents affect methane distribution, however, currents transport the methane, but do not decrease the concentration as no concentration gradient is included in the equation of the advective flux. Largier (2003) put it that way: "The diffusive flux is then determined by the "eddy diffusivity" K that parameterizes the strength of small-scale motions and acts to smooth out gradients (whereas advection simply displaces them)." and also "advection is the mean movement and diffusion is the spreading out." We drew a sketch to show the influence of advection/currents (Fig. 1 in the response to reviewer 2) showing that independent of the current velocity, the vertical concentration profile would always look similar: the concentration would exponentially decrease with distance to the seafloor. In addition, the seasonal thermocline will always limit vertical transport, thus, the model is qualitatively correct, but not necessarily quantitatively.

3) The description of the turbulent diffusion seems to me not correct. Fick law of diffusion handles molecular diffusion with only the concentration gradient as driving force. In the case of methane in the North Sea I think that eddy covariance calculations would be more appropriate. The cited literature of Largier 2003, seems to be not appropriate as it is dealing with the distribution of particles and not dissolved molecules by advection!! and diffusion. There are some studies modelling the methane distribution in shallow sea, however they are using numeric modelling. Grunwald, M., Dellwig, O., Beck, M., Dippner, J. W., Freund, J. A., Kohlmeier, C., . . . Brumsack, H.-J. (2009). Methane in the southern North Sea: Sources, spatial distribution and budgets. *Estuarine, Coastal and Shelf Science*, 81(4), 445-456. Wahlström, I., & Meier, H. E. M. (2014). A model sensitivity study for the sea-air exchange of methane in the Laptev Sea, Arctic Ocean. *Tellus B*, 66, 24174.

Author reply 3: Fick's law is not only used for molecular diffusion, but also for eddy or turbulent diffusion in the ocean or large lakes. Wahlström, I., & Meier, H. E. M. (2014) used also turbulent diffusion and a reservoir to calculate the change of concentration over time and depth, similar to our approach; they wrote:

$$\frac{\partial \phi}{\partial t} + W \frac{\partial \phi}{\partial z} = \frac{\partial}{\partial z} \left(\Gamma_{\phi} \frac{\partial \phi}{\partial z} \right) + S_{\phi} \quad (1)$$

where ϕ is the dependent variable (methane concentration in our case), t time, z vertical coordinate, W (m s^{-1}) vertical water velocity, Γ_{ϕ} ($\text{m}^2 \text{s}^{-1}$) the exchange coefficient (also named diffusion coefficient) and S_{ϕ} is the source and sink term for the dependent variable. The first term to the right represents turbulent diffusion and is according to Fick's first law. In this paper and also by Soetaert and Herman (A practical guide to ecological modelling, 2009, Springer) is stated that turbulent eddy diffusion applies not only for particles, but also for molecules.

The turbulent diffusion coefficient is much larger than the molecular diffusion coefficient (diffusion in water (molecular) $\sim 10^{-11} - 10^{-7} \text{ m}^2/\text{s}$, vertical diffusion in the ocean, $k_z \sim 10^{-5} - 10^{-3} \text{ m}^2/\text{s}$, horizontal diffusion in the ocean, $k_x \sim 1 - 1000 \text{ m}^2/\text{s}$). Largier (2003) was cited as we used the horizontal diffusion coefficients reported in this paper. Largier wrote: "Further, a comparison of different studies indicates an exponential increase in K_y with distance from the shore (Fig. 3A): in wave-driven nearshore waters ($y \sim 0.1 \text{ km}$) values on the order of $1-10 \text{ m}^2/\text{s}$ are found (Smith and Largier 1995), whereas values on the order of $100 \text{ m}^2/\text{s}$ are found over the wind-driven shelf ($y \sim 10 \text{ km}$; Davis 1985, Largier et al. 1993), and much larger values on the order of $1000 \text{ m}^2/\text{s}$ or greater are found in the offshore waters of the California Current ($y \sim 100-1000 \text{ km}$; Swenson and Niiler 1996)."

Eddy covariance is, as far as we know, applied in the atmosphere to calculate vertical turbulent fluxes within atmospheric boundary layers. This technique is also used to derive benthic oxygen fluxes

between seafloor and overlying water. Covariance means that two variables vary, wind and concentration vary in the atmosphere, oxygen concentrations and vertical velocity vary near the seafloor in the case of oxygen fluxes. Both variables are measured. What we have are vertical methane concentration profiles, but no measurements of vertical displacement. Therefore, we cannot use this technique. Furthermore, Sundermeyer and Price (1998) wrote: "Put another way, mixing processes are those which can (or must) be modeled by diffusion, i.e., molecular or very small-scale advective processes in which individual exchange events are not resolved, while stirring processes are resolved events, e.g., the streaking and folding of a tracer within a resolved eddy field."

Kinetics of MOx I cannot follow the conclusion that MOx rates are low. The MOx rates from this study lay well within the range of other marine areas, as the authors state. And even a comparison of the turnover times, which is independent from the M.conc. show that data from this study (100 d) are comparable with 80 - 1000 d from Gentz et al 2013, or 127 - 455 d from the Baltic Sea (Jacobs et al 2013). There are two ways of calculation k' the first order constant. It can be obtained via arithmetic, i.e. calculation the average or median of the single measurements or – as suggested by the authors – graphically i.e. the slope of the linear regression. However, if using the latter one has to prove / test the linearity of the relation and give as well the confidence interval of the regression line. But no matter how k' was calculated, it still will be only k' in the end.

Author reply 4: The reviewer is completely right that k' is still k' in the end, no matter how one derives the value. We could have also just taken the average of all k' and state the turnover time of 100 d to point out that the activity of methane oxidizing bacteria is low. Our main point is that high MOx-rates do not indicate a highly active methane oxidizing bacterial community. If one has a k' of 0.01 d^{-1} , but different methane concentrations, e.g. 1000 nM and 1 nM, then one would get MOx-rates of 10 nM/d and 0.01 nM/d, respectively. The former suggests a fast consumption of methane whereas the latter a slow consumption, but actually the uptake rate of methane (or the activity of the bacteria) is the same.

The authors also use data from literature of the K_m and a range of marine Mox rates to interpolate a Michaelis Menten kinetics. However, the methane concentrations of this study are in very low range and not even near the half-saturation concentration ($1 - 12 \text{ M} = 1.000 - 12.000 \text{ nM}$). For a kinetic study to obtain v_{max} or K_m much more data with a broader range of Mconc are needed. See also Lofton et al 2014. Thus I do not follow the interpolated values of v_{max} and K_m given in the text and in figure 7.

Author reply 5: In Fig. 7A we show the range of kinetically possible uptake of methane by methanotrophs using K_m and maximum MOx-rates published in literature. This figure shows that methane oxidation ranges from a rapidly increasing uptake of methane as soon as methane is available (MM1) to a slowly increasing methane-uptake although methane concentrations reach high values (MM2).

In Fig. 7B we fit a MM-curve to our data, that is, we adjusted K_m and v_{max} starting with the MM2-values until a good fit was reached. As noted in the response to the first reviewer having a related comment; the fitted curve has a R^2 of 0.81 in the range of our data. However, the reviewer is right that there is no proof beyond K_m . Therefore, we rewrote the section and include a linear fit to the data assuming that we are in the linear range of the MM-kinetics based on the literature values (Page 15, Line 518). The linear fit gives a k' value of 0.01 d^{-1} with an R^2 of 0.82. However, this k' is based on 120 measurements instead of only replicates ($n=2-3$) or a time series ($n=6-9$). Therefore, k' is still k' but statistically more precise.

Please also note the supplement to this comment: <http://www.biogeosciences-discuss.net/11/C8517/2015/bgd-11-C8517-2015-supplement.pdf>

How much water was filtered? This would be important to know to explain the failure of the PCR to detect any methanotrophs.

Author reply 6: A similar comment was raised by reviewer 1. Here is our response: We think that our DGGE-results are reliable, because we filtered 8 L of water, had good DNA-extracts, and used sufficient DNA for PCR. The quality of the winter samples was not as good as the quality of the summer samples, but from our experience with pelagic samples, the results are plausible, too.

I do not think that Ficks first law is valid here. It deals with molecular diffusion, assuming no turbulence or water movement. I think turbulent, eddy correlation would be more appropriate here. Furthermore, I do not see why this diffusion (if any) would only occur in two directions (west and east) but not north and south. So, the two dimensional assumption is difficult to support in a three dimensional water column.

Author: see reply 3 above

As I am not really convinced of the validity of the basic model (see above) I do not comment on the further application of this model.

Author: We described the validity of the equations in reply 3 above, which are the fundamentals of the model.

But in section 3.1 you state that there was no influence of the tides on the seepage intensity ????

Author reply 7: That is correct and the UWMS-data confirm this statement.

It would be nice to have a contour plot of the MOX-rates as well, for better comparison with the methane concentrations.

Author reply 8: Figure 8 shows the direct comparison of methane concentration and methane oxidation rates, thus, we think that a contour plot of MOX-rate data is not necessary. Moreover, we don't have a sufficient comprehensive data set of MOX-rates that would result in a reliable contour plot. Measurements were performed in five distinct water depth at each station and were partly excluded as some measurements were below the limit of detection.

But this is very strange if more methane is added to the sample, one would expect higher oxidation rate, but they seem to be lower than the ^3H -rates??? I suggest omitting the ^{14}C -data.

Author reply 9: We found similar results in Storfjorden, Svalbard (Mau et al., 2013). There, we suggested that the methane-oxidizing-community is not capable to consume more methane and, thus, cannot utilize the additional high methane load provided if using ^{14}C - CH_4 adding ~500 nM in contrast to adding about 2-3 nM in the case of ^3H - CH_4 . In this paper, we further proposed that the use of ^{14}C - CH_4 as tracer allows to identify if methane oxidizing microorganisms in a water mass are capable to consume elevated methane concentrations or not.

This is an unexpected finding. Did the authors run positive controls to be sure that the PCR was working at all? How much water was filtered on the filter?

Author: see reply 6 above

But a lower seepage rate in winter would also lead to lower methane concentrations...

Author reply 10: Certainly, the seepage rate can be variable in time. However, the gas flare observations shown in the paper are observations of seepage in the winter that indicate an intense seepage although dissolved methane concentrations are low.

Figure 2: numbers for the clusters are much too small!, correct July 2013 (S12-20) and January 2014 (W2-12)

Author reply 11: We changed the number size and figure caption accordingly.

Figure 4: Are there 2 stations with 0 km? In the figure there are different sampling depth for the eastern and western transect. But three scales for 4 figures are too much. You could try with a log-scale or two scales with some data above or below the scale.

Author reply 12: Yes, there are two stations at 0 km as described in the method section. We corrected the different depth scales, but think that less scales for methane concentrations would decrease the information provided by the measurements.

Figure 5: It would be nice to show the MOX-rates in the same way as the Mconc in figure 3. Thus it would be more evident where the MOX-rates are elevated. As pointed out in the discussion, the

turnover time or k' are also important parameters, thus it would be nice to also depict them. The figure on the linearity of the incubation time is a basic assumption and could go to the supplementary info.

Author reply 13: Please refer to the reply 8 above for illustration of MO_x -rates. We included a supplementary figure that shows the measured k' (Supplementary Material 6). We included the figure of the time series to show that only a small amount of the tracer was oxidized by microorganisms over four days suggesting a slow uptake of methane and confirming our hypothesis that microbial methane oxidation is a small sink of methane in the research area.

Interactive comment on “Seasonal methane accumulation and release from a gas emission site in the central North Sea” by S. Mau et al.

J. Kessler (Referee)

john.kessler@rochester.edu

Received and published: 13 February 2015

The authors provide a straightforward and clean analysis of the methane dynamics at a relatively shallow seep site in the central North Sea. Methane concentration and oxidation rates are provided and used with some modeling investigations to constrain seasonal changes in mixing, oxidation, and air-sea flux. The manuscript finds that (1) summer stratification allows methane to accumulate in the deeper waters, (2) methane oxidation is a minimal sink of methane during all seasons, (3) there is likely an enhanced release to the atmosphere following the termination of summer stratification, and (4) dispersion largely causes methane concentrations to decrease.

My specific comments focus on two main issues: sampling/measurements and explanation of conclusions.

Sampling/Measurements: 1) I would have liked more explanation on the air-sea flux measurements. For example, was the concentration of methane measured in the atmosphere directly or are average atmospheric values used in your calculations? If you are collecting atmospheric samples for methane analysis, at what height about the sea surface are you collecting the samples? At what height above the sea surface did you measure wind speed and did you correct for a 10 m height?

Author: The atmospheric value was calculated using the Bunsen solubility and measured ocean temperature and salinities. Wind speed was measured 22 m above sea level onboard. We forgot to correct the value, but use the power law $V_h/V_{10}=(h/10)^{0.13}$ to do this. The corrected values are included in Fig. 8, but they do not alter our interpretation. Thanks for pointing out this issue (Page 9, Line 289-290).

Also, I'm slightly concerned about the possibility of under-sampling the surface waters for methane concentration. Is there a possibility that elevated dissolved concentrations of methane in the surface waters

were contained in fairly isolated plumes and thus you simply did not sample these regions? While using continuous, underway air-sea flux systems would have been nice (e.g. Du et al., Environmental Science & Technology, 2014) for a more comprehensive data set, a bit more discussion to justify that your discrete sampling was representative of this seep region would be helpful.

Author: Our intention was to compare the different fluxes. Although we have only a summer and winter snapshot picture based on a few discrete samples, still it is certain that e.g. wind speed is higher in winter and methane concentrations are lower in winter due to the enhanced mixing by wind. Therefore, the ratio of the flux estimates allow an evaluation of the importance of the different transport and loss processes of methane. A comprehensive data set such as the one you mentioned is needed to really quantify the sea-air flux and such an investigation would be necessary to be conducted at different wind speeds and covering a larger area. We included a more detailed discussion in a revised version (Page 17, Line 564-573).

2) The authors do not provide any data on current velocity. ADCP data would have been beneficial and would have helped to determine if turbulent mixing is significant. For example, on page 18023, line 7-8, the authors state that "The advective transport by ocean currents was not estimated as this process does not decrease the concentration of methane, but solely transports methane from the seep site in direction of the current flow." That is only true if advective transport is uniform. Differences in current velocity and direction with depth would lead to turbulent mixing. These processes may be contained in your vertical and horizontal eddy diffusion, but a bit more discussion on the magnitude and direction of the currents throughout the water column would have been beneficial.

Author: The second reviewer also suggested to present current measurements, although, as you pointed out, the turbulent mixing is included in the eddy diffusion. Unfortunately, we don't have any ADCP-measurements, solely modelled data by the Bundesamt für Seeschifffahrt und Hydrographie (BSH) using wind and air temperature forecasts. However, we included a description and add a plot to the supplementary material showing the east-west and north-south velocities of the currents during the sampling campaigns (Page 10-11, Line 348-355). We also included an estimate of the advective transport (Page 8, Line 251-262, Page 16, Line 550-556).

Both of my comments on the "Sampling/Measurements" above are meant to provide clarity to the reader. I do not anticipate they will change the conclusions of this manuscript significantly.

Conclusions: 1) Perhaps the most impactful finding of this manuscript is that methane oxidation was not a large sink of methane. I am very curious to learn more about why this is, especially during summer stratification. Do the authors have access to nutrient or trace metal data to suggest why this may be? From a different perspective, what increase would the authors have expected in the average k' value for methane oxidation during summer stratification? The lack of an increase in the k' values for methane oxidation is a significant discovery but without any explanation as to why this is occurring makes the manuscript feel incomplete.

Author: Similar to the finding of Tavormina et al., 2013, who observed that there is not a strong correlation between methane concentrations and putative methanotrophs, we also find that there is no strong correlation between methane concentrations and activity of methane oxidizing microorganisms. We agree with these authors that either these putative methanotrophs are facultative methanotrophs, not necessarily dependent on methane, or that there is a limitation by e.g. trace elements, which are mainly limited in the upper ocean. We included such a statement for completion (Page 20, Line 693-697).

In conclusion, this is a strong manuscript that makes quality measurements of methane dynamics and does a meaningful interpretation of the data. I doubt that any of my comments will lead to significant modifications to the conclusions in this manuscript. Nonetheless, they would provide a bit of clarity to the interested reader. I enjoyed reading this manuscript.

1 **Seasonal methane accumulation and release from a gas emission site in the central North Sea**

2

3 S. Mau^{1*}, T. Gentz², J.-H. Körber¹, M. Torres³, M. Römer¹, H. Sahling¹, P. Wintersteller¹, R. Martinez²,
4 M. Schlüter², E. Helmke²

5 ¹ MARUM – Center for Marine Environmental Sciences and Department of Geosciences, University of
6 Bremen, Klagenfurter Str., 28359 Bremen, Germany

7 ² Alfred-Wegener-Institute for Polar and Marine Research, Am Handelshafen 12, 27570
8 Bremerhaven, Germany

9 ³ College of Oceanic and Atmospheric Sciences, Oregon State University, 104 Ocean Admin Building,
10 Corvallis, Oregon 97331-5503

11

12 * Corresponding author: Susan Mau, e-mail: smau@marum.de

13

14 Abstract

15 Hydroacoustic data document the occurrence of 5 flare clusters and several single flares from which
16 bubbles rise through the entire water column from an active seep site at 40 m water depth in the
17 central North Sea. We investigated the difference in dissolved methane distributions along a 6 km
18 transect crossing this seep site during a period of seasonal summer stratification (July 2013) and a
19 period of well mixed winter water column (January 2014). Dissolved methane accumulated below
20 the seasonal thermocline in summer with a median concentration of 390 nM, whereas during winter,
21 methane concentrations were much lower (median concentration of 22 nM) and punctually elevated
22 due to bubble transport. High resolution methane analysis by an underwater mass-spectrometer
23 confirmed our summer results and were used to document prevailing stratification over the tidal
24 cycle. Although sufficient methane was available, microbial methane oxidation was limited during
25 both seasons. Measured and averaged rate constants (k') were on the order of 0.01 day⁻¹, equivalent
26 to a turnover time of 100 days. Time series measurements indicated a **microbial** uptake of only 5-6%
27 of the gas after 4 days, and no known methanotrophs and pmoA-genes were detected. Estimated
28 methane fluxes indicate that horizontal transport rapidly disperses dissolved methane, vertical
29 transport becomes dominant during phases of high wind speeds, and relative to these processes,
30 microbial methane oxidation appears to be low. To bridge the discrete field data we developed a 1D
31 seasonal model using available year-long records of wind speed, surface temperature and
32 thermocline depth. The model simulations show a peak release of methane at the beginning of fall
33 when the water column becomes mixed. Consistent with our field data, inclusion of microbial
34 methane oxidation does not change the model results significantly, thus microbial oxidation appears

35 to be not sufficient to notably reduce methane during summer stratification before the peak release
36 in fall.

37

38 1 Introduction

39 Methane is, after water vapor and CO₂, the most important greenhouse gas. Its concentration has
40 increased by a factor of 2.5 since preindustrial times, from 722 ppb in 1750 to 1800 ppb in 2011
41 (IPCC, 2013). The total global emission was estimated to be ~550 Tg (methane) yr⁻¹ with an
42 anthropogenic contribution of 50 to 65%. Geological sources, which were not considered in IPCC
43 reports previously, are suggested to account for up to 30% of total emissions and include
44 anthropogenic emissions related to leaks in the fossil fuel industry as well as natural geological seeps
45 both terrestrial and marine (IPCC, 2013). An improved emission estimate from marine seeps suggests
46 that these sources contribute ~20 Tg methane yr⁻¹, i.e., 4% of the global emissions, to the
47 atmospheric methane (Etiope et al., 2008).

48

49 In general, oceans have been found to be a minor source of methane to the atmosphere, accounting
50 for 2-10% of the global emissions (Bange et al., 1994). A major fraction of the oceanic source (75%) is
51 thought to originate from estuaries, shelf and coastal areas (Bange, 2006; Bange et al., 1994). For
52 example, the European coastal areas were found to emit 0.46-1 Tg yr⁻¹, and thus contribute
53 significantly to the overall global methane oceanic emissions (Bange, 2006). The author, however,
54 points out that this estimate underestimates the coastal input, since fluxes from estuaries and
55 shallow seeps are not adequately represented. Moreover, there is growing evidence that methane
56 release from natural seepages and abandoned boreholes can significantly contribute to the global
57 atmospheric methane emissions, especially from the North Sea (Judd et al., 1997; Rehder et al.,
58 1998; Schroot et al., 2005).

59

60 It is important to consider shelf and coastal areas, as they are regions where most organic matter is
61 deposited. Although continental margins account for only 10% of total ocean area and 20% of total
62 ocean primary production (Killops and Killops, 1993), more than 90% of all organic carbon burial
63 occurs in sediments depositing on deltas, continental shelves, and upper continental slopes (Berner,
64 1989). At these locations, which are also characterized by high sedimentation rates, organic carbon is
65 rapidly buried beneath the sulfate reduction zone, and becomes available to methanogens (e.g.
66 Cicerone and Oremland, 1988). Methane is also generated by thermal breakdown at high
67 temperature and pressure. A significant fraction of the formed methane is oxidized in anaerobic and
68 aerobic sediments (e.g. Boetius et al., 2000; King, 1992), the remaining methane may be transported
69 into the overlying water either dissolved in upwardly advecting pore waters or in case of

70 oversaturation, in the form of gas bubbles. Because methane is undersaturated in seawater, rising
71 methane bubbles partially dissolve during ascent through the water column (McGinnis et al., 2006),
72 where the dissolved methane may be further consumed by microbial oxidation. Only if this methane
73 survives transport to the mixed layer, can it be transferred to the atmosphere.

74
75 Using a bubble dissolution model in combination with acoustic observations of rising bubbles,
76 McGinnis et al. (2006) showed that only bubbles emitted at shallow seeps (<100 m) may reach the
77 atmosphere. Methane rich bubbles from deeper seeps fully dissolve in the ocean. Model simulations
78 based on methane concentrations, oxidation rates, and current records of two plumes observed in
79 the Santa Barbara Basin indicate that half of the dissolved methane reaches the atmosphere and the
80 other half is microbially oxidized of the shallow plume whereas the deeper plume is mostly oxidized
81 (Mau et al., 2012). Thus, depending on the emission depth, methane remains in the ocean and can
82 be microbially oxidized.

83
84 Shallow seeps thus are likely more important contributors to atmospheric methane. However, even
85 at shallow seeps, density stratification may limit the vertical transport. For example, at the 70 m
86 deep Tommeliten area in the North Sea, less than ~4% of the gas initially released at the seafloor
87 reaches the mixed layer during summer, because a seasonal thermocline constrains methane
88 transport to the atmosphere (Schneider von Deimling et al., 2011). Summer stratification traps
89 methane beneath the thermocline, some of which may be consumed by microbial oxidation, and
90 some will be released in the fall during first storm events. In order to investigate the seasonal cycle of
91 methane in the North Sea, we studied a shallow seep area both during summer (July 2013) when the
92 water column was stratified, and in winter (January 2014) when the water column was well mixed.

93 94 1.1 Study Site

95 The study site is situated in an area of active gas venting above a shallow gas reservoir in the central
96 North Sea. The gas vents are located in the Netherlands sector, license block B13 (Fig. 1). They occur
97 at shallow water depth (< 45 m) in a flat region that lacks any morphological expression typical of
98 seep structures (Schroot et al., 2005). These seeps are likely sourced from a biogenic methane
99 reservoir ($\delta^{13}\text{C}$ values of -80‰ VPDB) of Pliocene to Pleistocene age, which lies 600-700 m below the
100 seafloor. Patches of gas saturated sediments between the gas reservoir and the seafloor have been
101 imaged in seismic data. These data plus observations of separate bubble streams in the water
102 column and rapidly decreasing methane concentrations in cores with distance from the vent site led
103 Schroot et al. (2005) to describe our study site as a leaking gas reservoir with laterally discontinuous
104 seepage.

105
106
107
108
109
110
111
112
113
114
115
116
117
118
119
120
121
122
123
124
125
126
127
128
129
130
131
132
133
134
135
136
137
138
139
140

The seeps are located in the central North Sea, south of Dogger Bank, a sandbank with water depth 20 m shallower than in the surrounding sea. Water masses from the north (Atlantic Water) and south (Straits of Dover) meet (Kröncke and Knust, 1995) in this central area, where the general anticlockwise circulation along the coasts of the North Sea becomes weak and varied (Fig. 1, Howarth, 2001). The water above the sandbank is well-mixed throughout the year in contrast to the deeper waters surrounding the bank that become stratified during spring and summer. The front, where these waters encounter, bifurcates around the Dogger Bank and the location of the front is influenced by tidal current speed. Generally, tides have the strongest influence on currents in this region, followed by wind forcing (Howarth, 2001; Otto et al., 1990; Sündermann and Pohlmann, 2011).

Seasonal temperature stratification is a common feature in this and other shelf seas, and it separates high-light and low-nutrient surface water from low-light and high-nutrient bottom water. Even though in some shelf areas, the tidal energy is sufficient to overcome stratification, models by Pingree and Griffiths (1978) and Holt and Umlauf (2008) indicate that our study area is situated in a stratified region, east of the tidal front that surrounds the shallowest part of the Dogger bank. Thus, during spring and summer, the water column over the seeps investigated here, remains stratified over the course of a tidal cycle.

2 Methods

All data used in this study was collected during two cruises with *RV Heincke*. The first cruise (HE406) was conducted during summer 2013 (20.-24. July), the second cruise (HE413) during winter 2014 (13.-22. January).

2.1 EM710 flare imaging

During the winter cruise, we used a Kongsberg EM710 multibeam echosounder to map active gas emissions in the study area (Fig. 2). For the precise localization of individual flares, i.e., bubble streams in an echogram, the water column data were post-processed using the Fledermaus tools FMMidwater, DMagic, and the 3D Editor (© QPS). The origin of individual flares was identified as the point of highest amplitudes near the seafloor. The coordinates of these points were extracted using the FMGeopicker and subsequently plotted on top of the bathymetry using ArcGIS 10.2 (©ESRI).

For visualization of flare deflections and bubble rising heights, selected flares were extracted from the water column data as point data and edited using the 3D Editor of DMagic. The processed flares were plotted over the bathymetry data in a 3D-view.

141

142 2.2 Water column sampling

143 To identify the size and magnitude of the dissolved methane plume generated by the bubble
144 discharge, seawater was sampled along a transect crossing the active gas emission sites (Fig. 2). The
145 transect, which extends 3 km to the east and 3 km to the west from a bubbling location (cluster 1 in
146 Fig. 2) was sampled twice, once in summer 2013 and once in winter 2014. In both cases, the eastern
147 sector (5 stations) was sampled on one day (~3 h) and the western sector (5 stations) on another day
148 (~3 h), so that the center stations was sampled twice.

149

150 Water samples were collected with a CTD/bottle rosette for methane concentration, methane
151 oxidation rate, and molecular analyses. The rosette was equipped with twelve 5 L Niskin bottles, a
152 Sea-Bird SBE 911 plus CTD, and an SBE 43 oxygen sensor for online monitoring of salinity,
153 temperature, pressure, and dissolved oxygen. The data are archived in PANGAEA (doi:10.1594 /
154 PANGAEA.824863 and doi:10.1594 / PANGAEA.832334). Twelve different water depths were
155 sampled at each station for methane concentration analysis and 5 water depths for methane
156 oxidation rates. Additional casts were **conducted** to sample sufficient water for molecular analyses.

157

158 2.2.1 Methane concentration

159 For methane concentration analysis, samples were collected in 60 ml crimp-top glass bottles. All
160 sample bottles were flushed with 2 volumes of water and filled completely to eliminate bubbles.
161 Bottles were immediately capped with butyl rubber stoppers and crimp sealed. After adding 0.2 ml of
162 10 M NaOH to stop any microbial activity, a 5 ml headspace of pure N₂ was introduced into each
163 bottle as described in Valentine et al. (2001) and the samples were stored at 4 °C. One to two
164 aliquots of the headspace were analyzed to determine methane concentrations using a **gas-phase**
165 **chromatograph** equipped with a flame ionization detector. Analyses were performed both on board
166 and post cruise. Replicate analyses of samples yielded a precision of ± 5%.

167

168 2.2.2 Methane oxidation rates

169 Methane oxidation (MOx) rates were determined from ex situ incubations of water samples in 100
170 ml serum vials. Sampling and incubations were performed as described in Mau et al. (2013). Briefly,
171 duplicate samples were collected: the set of samples taken at all stations was treated with 50 µl of
172 ³H-labeled methane (160–210 kBq) in N₂, and a second sample set, which was collected at 5 stations
173 in July 2013, was treated with 10 µl of ¹⁴C-labeled methane (12–15 kBq). After shaking the bottles to
174 equilibrate the tracer with the water, the samples collected in summer 2013 were incubated at 10 °C
175 and those collected in winter 2014 at 9 °C. All samples were incubated in the dark for 24 h. After

176 incubation, the total activity ($^3\text{H-CH}_4 + ^3\text{H-H}_2\text{O}$) in 1 ml aliquots was measured by wet scintillation
177 counting, and the activity of $^3\text{H-H}_2\text{O}$ was measured after sparging the sample for >30 min with N_2 to
178 remove excess $^3\text{H-CH}_4$. Incubations with $^{14}\text{C-CH}_4$ were terminated by injecting 0.5 ml of 10 M NaOH. A
179 5 ml headspace was then added so that the remaining $^{14}\text{C-CH}_4$ accumulated in the headspace, while
180 produced $^{14}\text{C-CO}_2$ and ^{14}C biomass was trapped in the aqueous NaOH solution. $^{14}\text{C-CH}_4$ in the
181 headspace was combusted to $^{14}\text{C-CO}_2$, and $^{14}\text{C-CO}_3^{2-}$ was converted to $^{14}\text{C-CO}_2$ through acidification
182 with HCl. The produced $^{14}\text{C-CO}_2$ was trapped in a solution of methoxyethanol and phenylethylamine,
183 and the radioactivity was measured by wet scintillation counting.

184
185 MOx rates were calculated assuming first-order kinetics (Reeburgh et al., 1991; Valentine et al.,
186 2001):

$$187 \quad \text{MOx} = k' [\text{CH}_4] \quad (1)$$

189
190 where k' is the effective first-order rate constant calculated as the fraction of labeled methane
191 oxidized per unit time, and $[\text{CH}_4]$ is the in situ methane concentration. To verify first order kinetics we
192 conducted time series incubations and measured the tracer consumption after 1, 2, 3, and 4 days.

193
194 In addition, control samples were frequently taken and poisoned immediately after the addition of
195 the tracer. The mean (\bar{x}) and standard deviation (s) of all controls sampled during a cruise were
196 calculated and the limit of detection (LOD) was set as:

$$197 \quad \text{LOD} = \bar{x} + 3s \quad (2)$$

199
200 The LOD was 0.02 nM day^{-1} for the summer 2013 survey, 0.09 nM day^{-1} for the winter 2014 survey,
201 and $0.0005 \text{ nM day}^{-1}$ for the ^{14}C -methane survey in summer 2013.

202
203 The MOx values were also corrected for differences between in situ and incubation temperatures
204 (Supplementary Material 1).

205 206 2.2.3 Analysis of bacterial communities

207 The composition of the bacterioplankton assemblages was examined using denaturing gradient gel
208 electrophoresis (DGGE) based on the 16S rRNA gene as described in Mau et al. (2013). In short,
209 immediately after sampling, 8 L of water were filtered and bacterial cells were concentrated on
210 Nuclepore filters ($0.2 \mu\text{m}$ pore size). The filters were stored on board at $-20 \text{ }^\circ\text{C}$ and at $-80 \text{ }^\circ\text{C}$ post

211 cruise. DNA was extracted by an UltraClean Soil DNA Kit (MoBio Laboratories, USA). 16S rRNA gene
212 specific PCR was conducted using the forward primer GM5 plus GC-clamp and the reverse primer
213 907RM (Muyzer et al., 1993) under conditions described by Gerdes et al. (2005). The PCR products
214 (ca. 500 bp) were analyzed by DGGE according to the protocol of Muyzer et al. (1993). Clearly visible
215 bands of the DGGE gels were excised from the gel. The DNA was reamplified by PCR (Gerdes et al.,
216 2005) and sequenced. The 16S rRNA gene sequences were taxonomically assigned by SILVA Online
217 Aligner (Pruesse et al., 2012).

218

219 The presence of methane-oxidizing bacteria in the communities was checked by searching for genes
220 encoding the particulate methane monooxygenase (*pmoA*), a key enzyme of methanotrophs
221 (McDonald et al., 2008). The *pmoA*-gene-specific PCR reaction was conducted by using the primer set
222 “*pmoA*” and amplification conditions described in McDonald and Murrell (1997).

223

224 2.3 Methane concentration analysis by underwater mass-spectrometry (UWMS)

225 In addition to the conventional methane analysis, in situ methane concentrations were detected and
226 quantified with an UWMS (Inspectr200-200, Bell et al., 2007; Gentz et al., 2013; Schlüter and Gentz,
227 2008; Short et al., 2001; Wenner et al., 2004). The fast sampling frequency (≤ 2 s) of the UWMS
228 allows mapping and quantification of methane in much higher resolution than the commonly used
229 CTD/rosette-sampling technique. The instrument consists of a membrane inlet system (MIS), an
230 Inficon (Bad Ragaz, Switzerland) Transpector CPM 200 quadruple mass spectrometer, a Varian (Palo
231 Alto, USA) turbo pump, a roughing pump, a peristaltic pump (KC Denmark), an embedded PC, and a
232 microcontroller. The UWMS was partly redesigned to include a cooling system (Ricor, K508), which
233 lowers the detection limit for methane to 16 nM. The cooling system and the improvement of the
234 detection limit are described in detail by Gentz and Schlüter (2012) and Schlüter and Gentz (2008).
235 For reproducible gas permeation through the MIS, water is constantly heated to a steady
236 temperature of 50°C and pumped at a flow rate of 3 ml min⁻¹ along the membrane by an external
237 peristaltic pump.

238

239 The UWMS was deployed above the central gas seeps (cluster 1, Fig. 2) on 21.07.2013 (16:31 – 22:32
240 UTC) at five different water depths: just above the seafloor, 35 m, 28 m, 25 m, and 10 m. When the
241 system had reached the respective depth, the research vessel moved slowly along a rectangular
242 transect (~125 m S-N, ~150 m E-W, Fig. 2) surrounding the flares of cluster 1 (4°5.44'N, 55°18.36'E)
243 and towed the UWMS, which continuously measured the methane concentrations. Each of the depth
244 transects took about an hour and recorded 400-800 methane concentration values.

245

246 2.4 Estimation of methane fluxes

247 **Advection, horizontal** and vertical turbulent diffusion, sea-air flux, and microbial oxidation were
248 quantified for the upper (0-30 m) and lower water column (30-40 m) during summer stratification
249 (July 2013) and for the entirely mixed water column (0-40 m) in winter (January 2014).

250

251 **The advective flux (ADV) was calculated by multiplying methane concentration (C) and current**
252 **velocity (v):**

253

$$254 \text{ADV} = vC \quad (3)$$

255

256 **Methane concentrations were averaged above and below the thermocline in the case of the summer**
257 **results and throughout the water column in the case of the winter results. Current velocities refer to**
258 **the resultant velocities calculated from the u and v component of the velocity vectors**
259 **(Supplementary Material 2 and 3) and were averaged over the time period of sampling. The current**
260 **data were provided by the Bundesamt für Seeschifffahrt und Hydrographie (BSH)**
261 **(www.bsh.de/de/Meeresdaten/Vorhersagen/Vorhersagemodelle/index.jsp) and were modelled**
262 **using wind and air temperature forecasts.**

263

264 Turbulent horizontal and vertical diffusion (*Diff*) were calculated with Fick's first law of diffusion as
265 described in Mau et al. (2012):

266

$$267 \text{Diff} = D \left(\frac{\partial C}{\partial x} \right) \quad (4)$$

268

269 where *D* is the horizontal or vertical diffusion coefficient in $\text{m}^2 \text{s}^{-1}$. $\delta C/\delta x$ is the spatial concentration
270 gradient in nM m^{-1} , estimated between the center and the outermost stations in the case of
271 horizontal diffusion calculation, and the concentration gradient between the lower and upper water
272 column in the case of vertical diffusion, calculated only for summer 2013.

273

274 D_h , the horizontal diffusion coefficient, can range between 0.1 and $1000 \text{ m}^2 \text{ s}^{-1}$ (Largier, 2003;
275 Sundermeyer and Price, 1998) depending on the proximity to land. As the study area is located more
276 than 230 km from shore, we used a D_h of $1000 \text{ m}^2 \text{ s}^{-1}$ for our calculations. The vertical turbulent
277 diffusion coefficient (D_v) can vary between 10^{-3} and $10^{-6} \text{ m}^2 \text{ s}^{-1}$ depending on the energy in the water
278 column (wind, tides, etc.) and stratification (Denman and Gargett, 1983; Wunsch and Ferrari, 2004).
279 As a first approximation, we used $10^{-4} \text{ m}^2 \text{ s}^{-1}$, which is a common cited value across the thermocline.
280 The vertical eddy diffusion was estimated for all vertical profiles (all 10 CTD-stations).

281

282 The sea-air flux was calculated as:

283

$$284 \quad SAF = k_W(C_W - C_A) \quad (5)$$

285

286 where k_W is the gas transfer velocity in cm h^{-1} , C_W is the measured concentration of methane and C_A
287 is the methane concentration in atmospheric equilibrium, both in nM. We calculated k_W , which
288 depends on wind speed and the temperature-dependent Schmidt number of the gas, using
289 parameterization developed by McGillis et al. (2001). Wind speed was recorded 22 m above sea level
290 onboard and corrected to the standard height of 10 m. C_A was derived using the Bunsen solubilities
291 given by Wiesenburg and Guinasso (1979) and measured ocean temperature and salinities. The sea
292 air flux was calculated for surface water samples of all 10 stations sampled in summer 2013 and
293 winter 2014.

294

295 The oxidative loss (OL) was calculated by depth integration of the MOx rates:

296

$$297 \quad OL = \bar{x}_{MOx} z \quad (6)$$

298

299 where \bar{x}_{MOx} is the averaged MOx rate in nM day^{-1} over the depth interval z in m. The depth interval
300 is defined by the water stratification in the case of summer 2013 and covers the entire water depth
301 in the case of winter 2014. Integration was done for all vertical profiles.

302

303 2.5 Seasonal model

304 A non-steady state, 1D-model was developed to investigate the temporal evolution of methane over
305 a year. We considered an entirely mixed water column during the winter month, stratification
306 development during spring that lasted until early fall when the entire water column becomes mixed
307 again. Hence, we considered one water layer during fall-winter (0-40 m) and two layers (upper and
308 lower water column) during spring and summer. The initial model configuration was defined by the
309 dissolved methane concentration observed in January 2014 (17 nM, excluding punctual high
310 concentrations due to bubbles) and the transport and loss quantities calculated for the mixed water
311 column condition in this month. We set the methane flux from the seafloor to be equal to the *SAF*
312 estimate of January 2014. In daily time steps, the *SAF* and the vertical eddy diffusion were calculated
313 using Eq. 3 and 4 (above) and based on the amount of methane obtained in the previous time step.
314 The parameters: mixed layer depth, wind speed, and surface water temperature were kept constant
315 over a month, but then adjusted to the conditions of the following month. The mixed layer depth

316 was determined from archived CTD-profiles (Pangaea) collected in an area extending from 3-6°E and
317 54-56°N. Monthly mean wind speed was taken from the web-site: www.windfinder.com of the
318 Ameland Oil Platform (mean of data from Aug. 2010-Mar. 2014) and Forties/North Sea (mean of data
319 from Dec. 2012- Mar. 2014). Surface water temperatures were provided by the BSH.

320

321 3 Results

322 3.1 Seep locations

323 Echosounder data indicate bubble emission in the area of the sampled transect (Fig. 2). The center
324 station was located at a known gas bubble emission site or flare cluster, where several bubble
325 streams occur in close proximity to each other. We observed an additional four flare clusters near
326 the western sector of the transect, which displayed a similar seepage intensity as at the central seep
327 site. In contrast, no additional flares were found in the area of the eastern sector. Although
328 echosounder data point to bubbles rising to, or close to, the sea surface, no bubbles were visually
329 identified at the sea surface due to rough sea state in winter 2014, however, surfacing gas bubbles
330 were visually documented when the sea was calm in summer 2013. Seepage intensity showed no
331 obvious variation related to tidal cycles, i.e., pressure variations due to high or low tides, rather,
332 seeps were found to be active during all survey crossings.

333

334 3.2 Oceanographic setting

335 In summer (July 2013) a seasonal thermocline separated surface (0-30 m) from bottom water (30-42
336 m; Fig. 3). The surface water consisted of a 10 m thick mixed layer below which the temperature
337 decreased stepwise from 17.5 to 7°C in 30 m. Lower salinity was observed in 15 and 25 m depth,
338 which departed from the general 34.55. The stepwise decrease in temperature and the salinity
339 variations indicate the successive development of several pycnoclines driven by increasing sea
340 surface temperatures and less wind activity in spring and summer. The oxygen concentrations
341 increased from 220 µM at the surface to 240 µM at 30 m. In contrast to the surface water, the
342 bottom water had a homogeneous temperature of 7°C, a salinity of 34.63 PSU and contained less
343 oxygen (190 µM).

344

345 In winter (January 2014) the entire water column was mixed (Fig. 3). The water had a temperature of
346 7°C, a salinity of 34.85 PSU, a density of 27.3 kg m⁻³, and oxygen concentrations of 280 µM.

347

348 Modelled current data indicate a dominant north-west transport with velocities ranging between
349 0.06 and 0.27 m s⁻¹ (resultant velocity). In summer, the eastern part of the transect was sampled
350 when currents were directed to the north-west with an average velocity of 0.24 m s⁻¹ and the

351 western part was sampled when currents turned from north-west to south-west with an average
352 velocity of 0.19 m s^{-1} . In winter, the eastern part of the transect was sampled when water moved
353 north-east turning north-west with an average velocity of 0.22 m s^{-1} and the western part was
354 sampled when water also turned from north-east to north-west, but with an average velocity of 0.1
355 m s^{-1} .

356

357 3.3 Methane concentrations

358 Consistent with the two layer structure observed by the temperature/salinity data, methane
359 concentrations in summer 2013 also show a two layer distribution, with higher concentrations in the
360 bottom water relative to the surface values (Fig. 4A). Methane concentrations in the surface water
361 range from 3.9-517.8 nM with a median of 32.5 nM. Methane concentrations in the bottom water
362 range between 39.7 and 1627.7 nM with a median of 390.6 nM. Highest concentrations in the
363 surface water were found near the center station (170 nM), which decreased to the outermost
364 stations (to the west to 96 nM and to the east to 13 nM). However, the decrease is not continuous
365 due to the presence of bubble emission sites in the area. Similarly, in the bottom water the highest
366 methane concentrations were found at the center station (600-700 nM) decreasing unevenly
367 towards the outmost stations (200-300 nM). In both layers the methane concentrations exceed the
368 background concentration of $\sim 20 \text{ nM}$ as measured at a reference station, which was located 32 km
369 from the central station (Supplementary Material 4), and reported methane concentrations in
370 Grundwald et al. (2009). Even this background value is already oversaturated with respect to the
371 atmospheric equilibrium concentration of 2.3-2.9 nM (at the relevant T /S conditions, Wiesenburg
372 and Guinasso, 1979).

373

374 In winter 2014, much lower methane concentrations were found (Fig. 4B). Highest values were
375 observed near the center site with concentrations of up to 656.6 nM. But such high concentrations
376 decreased rapidly horizontally (within 1 km) and were not encountered during repeated
377 measurements at the same location. The median of all methane concentration measurements along
378 the transect is 22.4 nM, which is only slightly above the regional background concentration. In
379 general, methane concentrations indicate a patchy distribution as expected in an active seep area.

380

381 3.4 UWMS methane concentrations

382 During the cruise in summer 2013, the UWMS was deployed in the vicinity of gas flare cluster 1 (Fig.
383 2). Because the instrument was towed close to several bubble streams, the recorded methane
384 concentrations range over three orders of magnitude, from 0 to 2127 nM in surface water (transects
385 in 10 m, 25 m, 28 m) and from 259 to 2213 nM in the bottom water (transects in 30 m and 40 m) (Fig.

386 5). Nonetheless, the general pattern of lower methane concentrations in the surface and higher
387 concentrations in the bottom water observed by conventional methods (see section 3.3) is also
388 apparent in the UWMS-data. The median values of the records in 10 m, 25 m, and 28 m water depth
389 range from 54 to 402 nM and in 30 m and 40 m depth, the medians range from 512 to 793 nM.

390

391 The UWMS measured the methane during ebbing tides, where water levels fell from 0.18 to -0.27 m,
392 whereas CTD/rosette samples were collected during rising tides, when sea level height increased
393 from -0.21 to 0.06 m and from 0.04 to 0.16 m (Supplementary Material 5). Again, the general pattern
394 of lower concentrations in the surface and higher ones in the bottom water was apparent in all
395 stations, even though methane data were obtained during different tidal phases.

396

397 3.5 Methane oxidation

398 Similar to the distribution of methane and co-located oceanographic data, MOx rates in summer
399 2013 show a two layer pattern whereas MOx measured in winter 2014 are uniform throughout the
400 water column (Fig. 6 A, B). In summer, significantly less methane was oxidized in the surface water
401 relative to the bottom water. In the surface waters MOx-rates ranged between 0.04 and 92.64 nM
402 day⁻¹ with a median of 0.10 nM day⁻¹ and in the bottom water between 1.60 and 840.93 nM day⁻¹
403 with a median of 3.99 nM day⁻¹. The total range of both layers (0.04- 840.93 nM day⁻¹) exceeds the
404 range of MOx-rates observed during the winter survey (0.09-8.72 nM day⁻¹). The median of all MOx-
405 rates measured in January 2014 was 0.24 nM day⁻¹.

406

407 Time series and ¹⁴C-methane tracer incubations indicate a slow oxidation rate of methane over time.
408 Although the methane concentrations greatly differ during both seasons, only 5-6 % of the ³H-
409 methane tracer was utilized during 4 day of incubation (Fig. 6D). In the ¹⁴C-methane tracer
410 experiments, a significantly higher concentration of methane is added to the sample relative to the
411 ³H-methane tracer additions (Mau et al., 2013). However, even the elevated methane additions did
412 not lead to a higher methane utilization. The MOx-rates determined using ¹⁴C-methane tracer
413 additions range from 0.0009 to 0.04 nM day⁻¹ with a median of 0.003 nM day⁻¹ in the surface water
414 (Fig. 6C). In the bottom water, the values range from 0.05 to 0.53 nM day⁻¹, with a median of 0.16
415 nM day⁻¹. Even though the ¹⁴C-MOx-rates were lower than the ones obtained with the ³H-methane
416 tracer, in both cases the two layer structure was obvious for the summer 2013 situation.

417

418 3.6 Microbial communities

419 Molecular samples taken in summer 2013 show also a difference between surface and deep waters,
420 whereas winter 2014 samples indicate a homogeneous distribution of microorganisms (Fig. 7, Tab.

421 1). In summer 2013, different DGGE banding patterns reveal the changes in microbial communities
422 with depth. The surface water samples showed two strong bands (Fig. 7, bands 6, 7) that could be
423 affiliated to the *Rhodobacteraceae* and two bands that could be assigned to the *Cyanobacteria* /
424 *Synechococcus* clade (8, 9). The middle and bottom water samples were characterized by a strong
425 chloroplast band (2), but also showed bands affiliated to the *Rhodobacteraceae* (5, 6). In the bottom
426 water samples of the central station, we found an additional band, assigned to *Pseudoalteromonas*
427 (10). The gel pattern of the winter samples showed no significant bands. The sequences of the faint
428 bands excised were of low quality. Only two of the bands could be assigned to the *Rhodospirillaceae*
429 (12, 13).

430

431 Neither the summer nor the winter bacterial communities exhibited known methanotrophic
432 bacteria, even though the samples originate from an actively gas venting area. The absence of
433 methanotrophic bacteria was further supported by the negative results of the pmoA-PCRs that
434 targets a methanotroph molecular marker gene.

435

436 4 Discussion

437 4.1 Distribution of methane in summer and winter

438 Our highest dissolved methane concentrations measured in the bottom water reach magnitudes
439 similar to those observed at other shallow seep sites (Tab. 2). Our highest value of 1627.7 nM is
440 comparable to measurements near the Coal Oil Point seep field, Santa Barbara Basin, California (up
441 to 1900 nM, Mau et al., 2012), and it is higher than methane concentrations reported for the
442 Tommeliten, North Sea (268 nM, Schneider von Deimling et al., 2011), and offshore Svalbard, west of
443 Prins Karls Forland (524 nM, Gentz et al., 2013).

444

445 Even though gas bubbling was observed at the sea surface in summer months, the dissolved
446 methane at these and also at other vent sites is trapped beneath a thermocline or halocline, which
447 hampers further ascent of the dissolved methane to the atmosphere. The studied seeps are located
448 at a depth of 40 m and the dissolved methane plume was found beneath a seasonal thermocline. At
449 the Tommeliten seep site, the methane plume was also observed beneath the seasonal thermocline
450 (Schneider von Deimling et al., 2011) whereas the methane plume originating from the 245 m deep
451 seeps offshore Prins Karls Forland was confined to water depths beneath a local halocline (Gentz et
452 al., 2013). In the Baltic Sea, summer stratification also leads to accumulation of methane below the
453 thermocline (Gülzow et al., 2013). At all these sites, an enhanced release of methane to the
454 atmosphere is thought to occur upon erosion of stratification. In contrast, the dissolved methane
455 plume originating from seeps situated between 5 and 70 m at the Coal Oil Point is dispersed above

456 the thermocline within the mixed layer (Mau et al., 2012), and as such is not controlled by seasonal
457 stratification patterns.

458

459 Trapping and accumulation of dissolved methane beneath a thermocline is also well documented in
460 lakes and freshwater reservoirs, where thermal stratification separates methane-poor, surface water
461 from the methane-rich, but anoxic, bottom water in e.g. a shallow floodplain lake in south-eastern
462 Australia (Ford et al., 2002), in a polyhumic lake in southern Finland (Kankaala et al., 2007), in the
463 subtropical Lake Kinneret in Israel (Eckert and Conrad, 2007), and in eight freshwater reservoirs in
464 India (Narvenkar et al., 2013). The accumulated methane is released when water starts mixing driven
465 by enhanced wind forcing and lower temperatures.

466

467 Our results verify the assumption that in a seasonal stratified system, no methane accumulation
468 occurs in winter, when the water column is well mixed as indicated by vertical profiles of
469 temperature, salinity, and oxygen. During our winter field program, methane concentrations were
470 found to deviate only due to bubble ascent and were otherwise low and constant throughout the
471 water. The median winter concentration of 22 nM is similar to the background methane
472 concentrations of 20 nM reported by Grunwald et al. (2009) for the German Bight, but the
473 concentration is elevated relative to water originating from the Atlantic Ocean, which carries 2.5-3.5
474 nM of methane (Rehder et al., 1998) and to the methane background concentrations of <5 nM at
475 Tommeliten (Niemann et al., 2005; Schneider von Deimling et al., 2011).

476

477 4.2 Low methane oxidation

478 Measured MOx-rates at our study site lie at the upper end of MOx-rates previously reported, which
479 span over six orders of magnitude from 0.001-1000 nM day⁻¹ (Tab. 2 and summarized in Fig. 1 in Mau
480 et al., 2013). The rates measured in deep water samples during summer (median 3.9 nM day⁻¹, up to
481 840 nM day⁻¹) equal those observed in the Gulf of Mexico after the Deepwater Horizon event
482 (median 10 nM d⁻¹, up to 820 nM day⁻¹) (Valentine et al., 2010). Even winter time rates are high in
483 comparison to rates measured in the Eel River Basin, an area of hydrate dissociation (Valentine et al.,
484 2001) and match rates of the Coal Oil Point seep field in the Santa Barbara Basin (Mau et al., 2012;
485 Pack et al., 2011).

486

487 However, we note that in spite of the reported high MOx values, detailed analysis of the data reveals
488 an overall low activity of methane oxidizing microorganisms. This apparent contradiction arises from
489 the fact that the MOx-rate of a given sample is traditionally calculated by multiplying methane
490 concentration with the fraction of the tracer converted per unit time, i.e., k' - the first order rate

491 constant. At a given k' value changes in methane concentrations yield MOx-rates that are low or high
492 depending on whether methane concentrations are low or high. Thus high MOx-rates might just
493 reflect high methane concentrations, and not necessarily a rapid turnover rate. The constant k'
494 provides an indication of the relative activity in a water sample (Koschel, 1980), but it cannot be
495 viewed independently from methane concentration, as k' is derived from tracer conversion in a
496 sample with ambient methane concentration.

497

498 Alternatively, the MOx-rate can be plotted against methane concentration, following the approach
499 used by Michaelis Menten (MM) kinetics to describe the rate of a first order enzymatic reaction that
500 depends on one substrate, by relating the reaction rate (V) to the substrate concentration (S) (Fig. 8).
501 The model takes the form of the equation:

502

$$503 \quad V = v_{max} \frac{S}{(K_m + S)} \quad (7)$$

504

505 where v_{max} is the maximum uptake rate and K_m is the concentration at which the reaction rate is half
506 of v_{max} . As illustrated in Fig. 8, the enzymatic uptake can be very rapid as soon as methane is available
507 and levels off when enzyme saturation is reached (low K_m and high v_{max} , MM-kinetics 1). However, in
508 some systems the uptake can be very slow, and enzyme saturation is reached at very high methane
509 concentrations (high K_m and low v_{max} , MM-kinetics 2). K_m values of cultured and uncultured soil
510 methane oxidizing bacteria range between 0.8-12 μM (Baani and Liesack, 2008; Bender and Conrad,
511 1993). For v_{max} , we used MOx-rate maxima reported for oceanic environments, which range between
512 100-1000 nM day^{-1} (Mau et al., 2013). Using these wide data ranges, we depict the predictive
513 behavior using both end-member for MM kinetics. Apart from 7 data points, which were collected in
514 the bottom water close to flare cluster 1 (stations S12 and S13, Fig. 2), all other data points are close
515 to a curve that follows MM-kinetics 2, with high K_m value and low v_{max} , hence pointing to a generally
516 slow uptake and oxidation of methane.

517

518 As all methane concentrations of our data are below K_m , we can derive an overall k' value from the
519 slope of the linear regression (Fig. 8), which for our case is 0.01 day^{-1} . As expected this value matches
520 the majority of the measured k' values (median of summer data: 0.02 day^{-1} , median of winter data:
521 0.01 day^{-1} , Supplementary Material 6) as well as the value k' derived from the time series incubations
522 (0.01 day^{-1} , $n=4$). We pose that, rather than using MOx-rates, or k' values from individual samples, a
523 fit to the entire data set provides an effective way to generate an overall parameter k' , which best
524 reflects the ecosystem microbial activity. The inverse of the modelled k' gives a turnover time of 100
525 days suggesting a rather low activity of methane-oxidizing bacteria in both summer and winter.

526

527 The low activity of methane oxidizing microorganisms is further supported by time series
528 experiments, ¹⁴C-methane spike experiments, and molecular analysis of filtered matter from
529 seawater. Time series incubations show a slow uptake of methane over time, solely 5-6% of the
530 added ³H-methane-tracer was converted after 4 days. Even when we spiked the sample with
531 elevated ¹⁴C-methane concentrations of 400-500 nM, there was no additional substrate utilized after
532 incubation for one day, indicating that methane oxidizing microorganisms cannot rapidly consume
533 the additional methane. Consistently, DGGE and *pmoA* analysis did not reveal the presence of any
534 known methanotrophic bacteria or *pmoA*-genes. Either methanotrophs were only present in low
535 numbers and/or poorly matched to the used PCR primers and, thus, were not detected (Hansman,
536 2008). Other observations in shallow marine waters (< 200 m) in the Pacific, Atlantic, and the Gulf of
537 Mexico show also that canonical methanotrophs were not detectable, but revealed novel sequences
538 closely related to those coding for methane monooxygenase (Elsaied et al., 2004; Tavormina et al.,
539 2008; Tavormina et al., 2013; Valentine, 2011; Wasmund et al., 2009), an enzymatic hallmark of
540 aerobic methanotrophs.

541

542 4.3 Transport is faster than methane oxidation

543 Although a part of the methane flux to the atmosphere is supported by direct bubble-transport, a
544 component that is being constrained by video observations and gas bubble samples (T. Gentz,
545 personal communication, 2014), here, we focus on the fate of the dissolved methane fraction. When
546 methane enters the water column, it is transported by ocean currents and spreads by horizontal and
547 vertical eddy diffusion. Dissolved methane can then support methane oxidizing microorganisms and
548 if water with methane concentrations higher than saturation reach the mixed layer, methane will be
549 transferred into the atmosphere. In order to evaluate the relative importance of these transport and
550 loss processes, we estimated the advective transport, the horizontal and vertical eddy diffusion, sea-
551 air flux, and integrated the MOx-rates over the water depth (see methods). All fluxes were estimated
552 in units of nmol m⁻² s⁻¹. As shown in Fig. 9, we estimated summer fluxes for the bottom (30-43m) and
553 surface waters (0-30 m), using data collected in July 2013, and winter fluxes for the entire
554 unstratified water column (0-42m) using data from January 2014. The results show that advective
555 transport and the horizontal eddy diffusion are the dominant processes rapidly transporting and
556 diluting the emitted methane. The loss processes, i.e., sea air flux and microbial oxidation, are more
557 than 4-orders of magnitude lower than these horizontally directed processes. Our flux estimates
558 revealed that in summer more methane is transported via vertical diffusion into the surface water
559 than is oxidized in the bottom water. In the surface water, 50% is oxidized and the other 50% is
560 transferred into the atmosphere. In winter, the sea air flux removes more methane from the water

561 column due to increased wind speed. Overall the flux estimates indicate that diffusion (dilution of
562 the methane rich water with background ocean water) outcompetes microbial methane oxidation.

563
564 All of these flux estimates are snapshots based on a few discrete samples and may vary by up to one
565 order of magnitude. The estimates were determined as described by Mau et al. (2012), which
566 includes a detailed discussion of the uncertainties associated with the calculations. Briefly, the
567 uncertainty originates from the precision of the different measurements, assumed diffusion
568 coefficients, and the parameterization of the gas transfer velocity. The uncertainty does not include
569 any possible variations during the 3 h of sampling. However, as the overall environmental setting will
570 remain constant, e.g. with the establishment of a seasonal thermocline and higher wind speed during
571 winter, the trend indicated by the flux comparison persists despite the uncertainties. Advection and
572 horizontal diffusion of methane will remain consistently higher than vertical diffusion and methane
573 oxidation.

574
575 Our flux estimates suggest that microbial oxidation is of minor importance in the central North Sea.
576 Particularly during periods of high wind speed (fall and winter), more methane reaches the
577 atmosphere than is oxidized in the water. In summer when lower wind speeds prevail, methane
578 oxidation is similar in magnitude to the gas transfer to the atmosphere. Our findings are similar to
579 those reported by Scranton and McShane (1991), who conclude that methane oxidation constitutes a
580 relatively small sink for methane in the Southern Bight of the North Sea ($0.00023\text{-}0.3\text{ nM day}^{-1}$),
581 relative to methane losses to the atmosphere ($0.00026\text{-}7.5\text{ nM day}^{-1}$), which are highest during
582 periods of high wind speed. The data are consistent with estimates for the shallow Coal Oil Point
583 methane plume in the Santa Barbara Basin (Mau et al., 2012). There, 0.05 mol day^{-1} are oxidized in
584 the surface water and 0.03 mol day^{-1} are transferred to the atmosphere.

585
586 4.4 Modeled methane accumulation and flux to the atmosphere over a year

587 To extend our inferences based on 2 field programs to seasonal changes over an entire year, we
588 developed a 1D model using wind speed, sea surface temperature, and the depth of the mixed layer
589 defined by the depth of the thermocline. CTD data of the surveyed region were used to specify the
590 monthly development of the mixed layer depth, which develops in May and deepens until the entire
591 water column becomes mixed in September (Fig. 10D). The model focused on the sinks of dissolved
592 methane: sea air flux and microbial methane oxidation.

593
594 Three simulation were run. The first simulation included solely the vertical transport (sea air flux and
595 vertical eddy diffusion during stratification), the second tested the uncertainty of the first simulation

596 due to the most unspecified parameter, Dv , and the third simulation included the microbial methane
597 oxidation (Fig. 10A-C).

598
599 Model results of the first simulation, which do not include methane oxidation, illustrate the seasonal
600 changes in methane concentrations. With decreasing wind speed in spring, methane concentration
601 slowly rise in the water column; at the onset of stratification, most of the dissolved methane
602 accumulates in the bottom water, leaving the surface water as the only source of methane to the
603 atmosphere and, thus, reducing the methane concentrations in the surface water. As the
604 concentration gradient between bottom and surface increases, more methane is transferred to the
605 surface water by vertical eddy diffusion; that in combination with lower wind speeds in the summer
606 cause methane concentrations to increase in the surface water. In late summer, beginning of fall, the
607 mixed layer depth deepens due to increased wind forcing. Surface and bottom waters become
608 mixed, which leads to a peak in methane concentration in the entire water column. This is
609 transferred to the atmosphere by sea air exchange. Due to prevailing high wind speeds in fall and
610 winter, methane concentrations rapidly decrease to a background concentration level of 20 nM.

611
612 The first simulation is greatly dependent on the vertical diffusion coefficient Dv . This parameter could
613 be one order higher ($10^{-3} \text{ m}^2 \text{ s}^{-1}$) due to shallow water depth or one order lower ($10^{-5} \text{ m}^2 \text{ s}^{-1}$) due to
614 low wind speed especially in summer (Denman and Gargett, 1983; Wunsch and Ferrari, 2004). For
615 example, during the first sampling period in July 2013 a wind speed of 2-5 m s^{-1} was recorded
616 whereas the average value used for the month July in the model was 7 m s^{-1} . Therefore, we tested
617 the uncertainty of the model that results from the variability in Dv in the second simulation. The
618 results of these simulations show that the modelled trend would be exaggerated if transport is less
619 ($Dv = 10^{-5} \text{ m}^2 \text{ s}^{-1}$). That is, e.g. a larger methane peak is predicted at beginning of fall, which would be
620 smoothed if we were to use a higher Dv ($10^{-3} \text{ m}^2 \text{ s}^{-1}$). The best fit to the data is achieved using a Dv of
621 $10^{-4} \text{ m}^2 \text{ s}^{-1}$, which yields a methane concentration of 39 nM in the surface water for the month July,
622 similar to the median of the measurements, 33 nM. A methane concentration of 260 nM is predicted
623 for the bottom water, which is equivalent in magnitude to the median of our measurements, 390
624 nM.

625
626 In order to further evaluate this critical parameter, we estimated Dv according to the equation by
627 Osborn (1980):

628
629
$$Dv = Kz = \Gamma \frac{\epsilon}{N^2} \tag{8}$$

630

631 where Γ is the efficiency of mixing and assumed to be a constant of 0.2. We used published
632 dissipation rates of turbulent kinetic energy (ϵ) in stratified shallow shelf seas (Palmer et al., 2008;
633 Thorpe et al., 2008) and calculated the buoyancy frequency (N) from the available CTD-profiles. The
634 results indicate that Dv is in the order of 10^{-4} to $10^{-6} \text{ m}^2 \text{ s}^{-1}$ during stratification. However, this rough
635 approximation neglects hourly changes that can be already of one order of magnitude. For example,
636 Palmer et al. (2008) observed and calculated Kz to range between 10^{-4} and $10^{-5} \text{ m}^2 \text{ s}^{-1}$ over a tidal
637 cycle.

638
639 After obtaining an appropriate Dv ($10^{-4} \text{ m}^2 \text{ s}^{-1}$), which fits best to our methane concentration data, we
640 included methane oxidation in the third model simulation. For this, we subtracted the averaged
641 measured MOx rates from the surface and bottom water reservoirs. MOx was included in the surface
642 water all year round, but in the bottom layer (i.e., in case of stratification) MOx was considered only
643 when sufficient methane has accumulated, that is, for the month May we assume a negligible MOx in
644 the bottom water. The model results do not show any significant difference by comparison to the
645 first simulation (which included only transport) except for the month of June, when the model
646 predicts significant methane consumption by MOx in the bottom water. Due to this decrease of
647 methane concentration in the bottom water, the concentration difference between the surface and
648 bottom water is not as large anymore and less methane is transferred by vertical eddy diffusion into
649 the surface water. The simulation drives the concentration gradient to equilibrium, until the water
650 column becomes fully mixed. We note that the model predicts a similar quantity of methane
651 released to the atmosphere at the beginning of fall whether or not methane oxidation is included in
652 the simulation.

653
654 In summary, if Dv is below $10^{-4} \text{ m}^2 \text{ s}^{-1}$ over the entire stratification period, then a peak release of
655 methane occurs at the beginning of fall when the water column becomes mixed. Microbial methane
656 oxidation appears insufficient to significantly reduce methane before the gas is transferred into the
657 atmosphere.

658
659 The model does not take into account any temporal changes of methane emission. Furthermore, a
660 sensitivity analysis of the model shows that especially wind speed affects model results. 10% higher
661 or lower wind speed over the entire year would in- or decrease the annual flux by 28% or 23%,
662 respectively. Sea surface temperature is less influencing the model result with 1.5% change if the
663 temperature is 10% higher or lower throughout the year.

664
665 5 Conclusions

- 666 1. Observations at a shallow gas seep site in the central North Sea document methane
667 accumulation below the thermocline during summer stratification, but no methane
668 accumulation in the winter. Similar summer time results are presented by Schneider von
669 Deimling (2011) for the Tommeliten area in the northern North Sea.
- 670 2. Our seasonal model bridges our summer and winter field studies and predicts an enhanced
671 sea-air flux at the end of the stratification period. Such an elevated sea-air methane transfer
672 was measured in the Baltic Sea when wind forcing increased after the summer month,
673 breaking down the stratification (Gülzow et al., 2013). The seasonality in fluxes highlights the
674 importance of understanding the effect of seasonal changes on estimates based on short
675 field programs.
- 676 3. We show that MO_x rates alone cannot be used to characterize the ecosystem microbial
677 activity, as these values are scaled to the methane concentration. We instead propose the
678 use of an average k' value of all the data, as an indicator of microbial activity. Such
679 derivation generates a more realistic parameter than values based solely on replicate
680 samples and is similar to values obtained by work-intensive time series incubations.
- 681 4. The idea that trapping of methane in the bottom water makes it more available to microbial
682 oxidation could not be verified. Even though the residence time of central North Sea water is
683 about 1.5-2 years (Prandle, 1984; Ursin and Andersen, 1978) and thermal stratification
684 prevails for 4 months and could provide sufficient time to establish a methanotrophic
685 community, we were not able to identify these organisms in the water column. Doubling
686 times of planktonic marine methanotrophs are not known to the authors, **as few if any such**
687 **methanotrophs are currently available in culture**. However, if we assume a doubling time of
688 ~ 10 h as known from cultured methanotrophs (Baani and Liesack, 2008; Khadem et al., 2010)
689 or a doubling time of 3.5 days as was estimated after the Deep Water Horizon incident in the
690 Gulf of Mexico by Kessler et al. (2011), a methanotrophic community could potentially
691 develop in the central North Sea. Even if the doubling time of methanotrophs in the field was
692 even longer as nutrients and substrates can be limiting, still the residence time of the water
693 would permit growth. **Possible limitations of essential trace elements or that the methane**
694 **oxidizing microorganisms are facultative methanotrophs (Tavormina et al., 2013), i.e., not**
695 **necessarily depending on methane, might explain, why stratification over a summer season**
696 **of 4 months does not enhance methanotrophy sufficiently to significantly hamper methane**
697 **release to the atmosphere upon water column mixing.**

698
699
700

701 Author contribution

702 S. M. designed study, measured methane concentrations and methane oxidation rates, calculated
703 the fluxes, developed the model and carried out model simulations, wrote the manuscript

704 T.G., R. M., and M.S. deployed the UWMS and post-processed the data

705 J.-H. K., M. R., H. S., and P. W. collected and post-processed hydroacoustic data

706 M. T. interpreted methane oxidation rate data, edited manuscript

707 E. H. implemented and interpreted molecular analyses

708

709 Acknowledgement

710 We are indebted to the captain, crew, and scientific research party of the research vessel *Heincke* (cruise

711 HE406 and HE413), especially to the organizer Sabine Kasten and Gerhard Bohrmann. We like to thank Sven

712 Klüber, Eva Kirschenmann, and Monika Wiebe for their help collecting and analyzing samples on board and in the

713 laboratory. We are grateful to Tessa Clemes from Alfred-Wegener-Institute for Marine and Polar Research

714 (Bremerhaven, Germany), who implemented the microbial analyses. We like to thank Antje Boetius, Gunter

715 Wegener, and Mirja Meiners from the Max Planck Institute for Marine Microbiology (Bremen, Germany) for

716 providing scientific equipment and laboratory support for oxidation rate measurements. This work is part of the

717 DFG project 'Limitations of Marine Methane Oxidation' (MA 3961/2-1).

718

719

720

721

722

723

724

725

726

727

728

729

730

731

732

733

734

735

736 References

- 737 Baani, M. and Liesack, W.: Two isozymes of particulate methane monooxygenase with different
738 methane oxidation kinetics are found in *Methylocystis* sp. strain SC2, *PNAS*, 105, 10203-10208, 2008.
- 739 Bange, H. W.: Nitrous oxide and methane in European coastal waters, *Estuar. Coast. Shelf S.*, 70, 361-
740 374, 2006.
- 741 Bange, H. W., Bartell, U. H., Rapsomanikis, S., and Andreae, M. O.: Methane in the Baltic and North
742 Seas and a reassessment of the marine emissions of methane, *Global Biogeochem. Cy.*, 8, 465-480,
743 1994.
- 744 Bell, R. J., Short, R. T., Van Amerom, F. H. W., and Byrne, R. H.: Calibration of an in situ membrane
745 inlet mass spectrometer for measurements of dissolved gases and volatile organics in seawater,
746 *Environ. Sci. Technol.*, 41, 2007.
- 747 Bender, M. and Conrad, R.: Kinetics of methane oxidation inoxic soils, *Chemosphere*, 26, 687-769,
748 1993.
- 749 Berner, R. A.: Biogeochemical cycles of carbon and sulfur and their effect on atmospheric oxygen
750 over Phanerozoic time, *Palaeogeogr. Palaeocl.*, 73, 97-122, 1989.
- 751 Boetius, A., Ravenschlag, K., Schubert, C. J., Rickert, D., Widdel, F., Gieskes, A., Amann, R., Jørgensen,
752 B. B., Witte, U., and Pfannkuche, O.: A marine microbial consortium apparently mediating anaerobic
753 oxidation of methane, *Nature*, 407, 623-626, 2000.
- 754 Cicerone, R. J. and Oremland, R. S.: Biochemical aspects of atmospheric methane, *Global*
755 *Biogeochem. Cy.*, 2, 299-327, 1988.
- 756 Denman, K. L. and Gargett, A. E.: Time and space scales of vertical mixing and advection of
757 phytoplankton in the upper ocean, *Limnol. Oceanogr.*, 28, 801-815, 1983.
- 758 Eckert, W. and Conrad, R.: Sulfide and methane evolution in the hypolimnion of a subtropical lake: a
759 three-year study, *Biogeochemistry*, 82, 67-76, 2007.
- 760 Elsaied, H. E., Hayashi, T., and Naganuma, T.: Molecular analysis of deep-sea hydrothermal vent
761 aerobic methanotrophs by targeting genes of 16S rRNA and particulate methane monooxygenase,
762 *Mar. Biotechnol.*, 6, 503–509, 2004.
- 763 Etiope, G., Lassey, K. R., Klusman, R. W., and Boschi, E.: Reappraisal of the fossil methane budget and
764 related emission from geologic sources, *Geophys. Res. Lett.*, 35, L09307, 2008.
- 765 Ford, P. W., Boon, P. I., and Lee, K.: Methane and oxygen dynamics in a shallow floodplain lake: the
766 significance of period stratification, *Hydrobiologia*, 485, 97-110, 2002.
- 767 Gentz, T.: Distribution and fate of methane released from submarine sources – Results of
768 measurements using an improved in situ mass spectrometer, 2013.doctoral thesis, Geosciences,
769 University Bremen, 173 pp., 2013.

770 Gentz, T., Damm, E., Schneider von Deimling, J., Mau, S., McGinnis, D. F., and Schlüter, M.: A water
771 column study of methane around gas flares located at the West Spitsbergen continental margin,
772 Cont. Shelf Res., doi: 10.1016/j.csr.2013.07.013, 2013. 2013.

773 Gentz, T. and Schlüter, M.: Underwater cryotrap-membrane inlet system (CT-MIS) for improved in
774 situ analysis of gases, Limnol. Oceanogr.: Methods, 10, 317-328, 2012.

775 Gerdes, B., Brinkmeyer, R., Dieckmann, G., and Helmke, E.: Influence of crude oil on changes of
776 bacterial communities in Arctic sea-ice, FEMS Microbiol. Ecol., 53, 129-139, 2005.

777 Grunwald, M., Dellwig, O., Beck, M., Dippner, J. W., Freund, J. A., Kohlmeier, C., Schnetger, B., and
778 Brumsack, H.-J.: Methane in the southern North Sea: Sources, spatial distribution and budgets,
779 Estuar. Coast. Shelf S., 81, 445-456, 2009.

780 Gülzow, W., Rehder, G., Schneider v. Deimling, J., Seifert, T., and Tóth, Z.: One year of continuous
781 measurements constraining methane emissions from the Baltic Sea to the atmosphere using a ship of
782 opportunity, Biogeosciences, 10, 81-99, 2013.

783 Holt, J. and Umlauf, L.: Modelling the tidal mixing fronts and seasonal stratification of the Northwest
784 European Continental shelf, Cont. Shelf Res., 28, 887-903, 2008.

785 Howarth, M. J.: North Sea Circulation. In: Encyclopedia of Ocean Sciences, Steele, J. H. (Ed.),
786 Academic Press, Oxford, 2001.

787 IPCC: Climate Change 2013 – The Physical Science Basis – Contribution of Working Group I to the
788 Fifth Assessment Report of the Intergovernmental Panel on Climate Change, Cambridge University
789 Press, Cambridge, 2013.

790 Judd, A. G., Davies, G., Wilson, J., Holmes, R., Baron, G., and Bryden, I.: Contributions to atmospheric
791 methane by natural seepages on the U.K. continental shelf, Mar. Geol., 140, 427-455, 1997.

792 Kankaala, P., Taipale, S., Nykänen, H., and Jones, R. I.: Oxidation, efflux, and isotopic fractionation of
793 methane during autumnal turnover in a polyhumic, boreal lake, J. Geophys. Res., 112, G02003, 2007.

794 Kessler, J. D., Valentine, D. L., Redmond, M. C., Du, M., Chan, E. C., Mendes, S. D., Quiroz, E. W.,
795 Villanueva, C. J., Shusta, S. S., Werra, L. M., Yvon-Lewis, S. A., and Weber, T. C.: A persistent oxygen
796 anomaly reveals the fate of spilled methane in the deep Gulf of Mexico, Science, 331, 312-315, 2011.

797 Khadem, A. F., Pol, A., Jetten, M. S. M., and Op den Camp, H. J. M.: Nitrogen fixation by the
798 verrucomicrobial methanotroph '*Methylacidiphilum fumariolicum*' SolV, Microbiology, 156, 1052-
799 1059, 2010.

800 Killops, S. D. and Killops, V. J.: An Introduction to Organic Geochemistry, Longman, Essex, United
801 Kingdom, 1993.

802 King, G. M.: Ecological aspects of methane oxidation, a key determinant of global methane dynamics,
803 Adv. Microb. Ecol., 12, 432-468, 1992.

804 Koschel, R.: Untersuchungen zur Phosphataffinität des Planktons in der euphotischen Zone von Seen,
805 *Limnologica*, 12, 141-145, 1980.

806 Kröncke, I. and Knust, R.: The Dogger Bank: a special ecological region in the central North Sea,
807 *Helgoländer Meeresunters.*, 49, 335-353, 1995.

808 Largier, J. L.: Considerations in estimating larval dispersal distances from oceanographic data, *Ecol.*
809 *Appl.*, 13, 71-89, 2003.

810 Mau, S., Brees, J., Helmke, E., Niemann, H., and Damm, E.: Vertical distribution of methane oxidation
811 and methanotrophic response to elevated methane concentrations in stratified waters of the Arctic
812 fjord Storfjorden (Svalbard, Norway), *Biogeosciences*, 10, 6267–6278, 2013.

813 Mau, S., Heintz, M. B., and Valentine, D. L.: Quantification of CH₄ loss and transport in dissolved
814 plumes of the Santa Barbara Channel, California, *Cont. Shelf Res.*, 32, 110-120, 2012.

815 McDonald, I. R., Bodrossy, L., Chen, Y., and Murrell, J. C.: Molecular ecology techniques for the study
816 of aerobic methanotrophs, *Appl. Environ. Microb.*, 74, 1305-1315, 2008.

817 McDonald, I. R. and Murrell, J. C.: The particulate methane monooxygenase gene *pmoA* and its use as
818 a functional gene probe for methanotrophs, *FEMS Microbiol. Lett.*, 156, 205-210, 1997.

819 McGillis, W., R., Edson, J., B., Ware, J., D., Dacey, J., W. H., Hare, J., E., Fairall, C., W., and Wanninkhof,
820 R.: Carbon dioxide flux techniques performed during GasEx-98, *Mar. Chem.*, 75, 267-280, 2001.

821 McGinnis, D. F., Greinert, J., Artemov, Y., Beaubien, S. E., and Wuest, A.: Fate of rising methane
822 bubbles in stratified waters: How much methane reaches the atmosphere?, *J. Geophys. Res.*, 111, 15,
823 2006.

824 Muyzer, G., de Waal, E., and Uitterlinden, A.: Profiling of complex microbial populations by
825 denaturing gradient gel electrophoresis analysis of polymerase chain reaction-amplified genes coding
826 for 16S rRNA, *Appl. Environ. Microbiol.*, 59, 695-700, 1993.

827 Narvenkar, G., Naqvi, S. W. A., Kurian, S., Shenoy, D. M., Pratihary, A. K., Naik, H., Patil, S., Sarkar, A.,
828 and Gauns, M.: Dissolved methane in Indian freshwater reservoirs, *Environ. Monit. Assess.*, 185,
829 6989–6999, 2013.

830 Niemann, H., Elvert, M., Hovland, M., Orcutt, B., Judd, A. G., Suck, I., Gutt, J., Joye, S., Damm, E.,
831 Finster, K., and Boetius, A.: Methane emission and consumption at a North Sea gas seep (Tommeliten
832 area), *Biogeosciences* 2, 335-351, 2005.

833 Osborn, T. R.: Estimates of the local rate of diffusion from dissipation measurements, *J. Phys.*
834 *Oceanogr.*, 10, 83-89, 1980.

835 Otto, L., Zimmermann, J. T. F., Furnes, G. K., Mork, M., Saetre, R., and Becker, G.: Review of the
836 physical oceanography of the North Sea, *Neth. J. Sea Res.*, 26, 161-238, 1990.

837 Pack, M. A., Heintz, M. B., Reeburgh, W. S., Trumbore, S. E., Valentine, D. L., Xu, X., and Druffel, E. R.
838 M.: A method for measuring methane oxidation rates using low-levels of ¹⁴C-labeled methane and
839 accelerator mass spectrometry, *Limnol. Oceanogr.: Methods*, 9, 245-260, 2011.

840 Palmer, M. R., Rippeth, T. P., and Simpson, J. H.: An investigation of internal mixing in a seasonally
841 stratified shelf sea, *J. Geophys. Res.*, 113, 2008.

842 Pingree, R. D. and Griffiths, D. K.: Tidal Fronts on the Shelf Seas Around the British Isles, *J. Geophys.*
843 *Res.*, 83, 4615-4622, 1978.

844 Prandle, D.: A modelling study of the mixing of ¹³⁷Cs in the seas of the European continental shelf,
845 *Philos. T. Roy. Soc. A* 310, 407-436, 1984.

846 Pruesse, E., Peplies, J., and Glöckner, F. O.: SINA: accurate high-throughput multiple sequence
847 alignment of ribosomal RNA genes, *Bioinformatics*, 28, 1823-1829, 2012.

848 Reeburgh, W. S., Ward, B. B., Whalen, S. C., Sandbeck, K. A., Kilpatrick, K. A., and Kerkhof, L. J.: Black
849 Sea methane geochemistry, *Deep-Sea Res.*, 38, S1189-S1210, 1991.

850 Rehder, G., Keir, R. S., Suess, E., and Pohlmann, T.: The multiple sources and patterns of methane in
851 North Sea waters, *Aquat. Geochem.*, 4, 403-427, 1998.

852 Schlüter, M. and Gentz, T.: Application of membrane inlet mass spectrometry for online and in situ
853 analysis of methane in aquatic environments, *J. Am. Soc. Mass Spectrom.*, 19, 1395-1402, 2008.

854 Schneider von Deimling, J., Rehder, G., Greinert, J., McGinnis, D. F., Boetius, A., and Linke, P.:
855 Quantification of seep-related methane gas emissions at Tommeliten, North Sea, *Cont. Shelf Res.*, 31,
856 876-878, 2011.

857 Schroot, B. M., Klaver, G. T., and Schuettenehelm, T. E.: Surface and subsurface expressions of gas
858 seepage to the seabed - examples from the southern North Sea, *Mar. Petrol. Geol.*, 22, 499-515,
859 2005.

860 Scranton, M. I. and McShane, K.: Methane fluxes in the southern North Sea: The role of European
861 rivers, *Cont. Shelf Res.*, 11, 37-52, 1991.

862 Short, R. T., Fries, D. P., Kerr, M. L., Lembke, C. E., Toler, S. K., Wenner, P. G., and Byrne, R. H.:
863 Underwater mass spectrometers for in situ chemical analysis of the hydrosphere, *J. Am. Soc. Mass*
864 *Spectrom.*, 12, 676-682, 2001.

865 Sundermeyer, M. A. and Price, J. F.: Lateral mixing and the North Atlantic tracer release experiment:
866 observations and numerical simulations of Lagrangian particles and a passive tracer, *J. Geophys. Res.*,
867 103, 21481-21497, 1998.

868 Sündermann, J. and Pohlmann, T.: A brief analysis of North Sea physics, *Oceanologia*, 53, 663-689,
869 2011.

870 Tavormina, P. L., Ussler III, W., and Orphan, V. J.: Planktonic and sediment-associated aerobic
871 methanotrophs in two seep systems along the North American Margin, *Appl. Environ. Microbiol.*, 74,
872 3985-3995, 2008.

873 Tavormina, P. L., Ussler, W., Steele, J. A., Connon, S. A., Klotz, M. G., and Orphan, V. J.: Abundance
874 and distribution of diverse membrane-bound monooxygenase (Cu-MMO) genes within the Costa Rica
875 oxygen minimum zone, *Environmental microbiology reports*, 5, 414-423, 2013.

876 Thorpe, S. A., Green, J. A. M., Simpson, J. H., Osborn, T. R., and Nimmo Smith, W. A. M.: Boils and
877 turbulences in a weakly stratified shallow tidal sea, *J. Phys. Oceanogr.*, 38, 1711-1730, 2008.

878 Ursin, E. and Andersen, K. P.: A model of the biological effects of eutrophication in the North Sea,
879 *Rapp. P.-v. Reun. Cons. Int. Explor. Mer*, 172, 366-377, 1978.

880 Valentine, D. L.: Emerging topics in marine methane biogeochemistry, *Annu. Rev. Mar. Sci.*, 3, 147-
881 171, 2011.

882 Valentine, D. L., Blanton, D. C., Reeburgh, W. S., and Kastner, M.: Water column methane oxidation
883 adjacent to an area of active hydrate dissociation, Eel River Basin, *Geochim. Cosmochim. Ac.*, 65,
884 2633-2640, 2001.

885 Valentine, D. L., Kessler, J. D., Redmond, M. C., Mendes, S. D., Heintz, M. B., Farwell, C., Hu, L.,
886 Kinnaman, F. S., Yvon-Lewis, S., Du, M., Chan, E. W., Tigreros, F. G., and Villanueva, C. J.: Propane
887 respiration jump-starts microbial response to a deep oil spill, *Science*, 330, 208-211, 2010.

888 Wasmund, K., Kurtboke, D. I., Burns, K. A., and Bourne, D. G.: Microbial diversity in sediments
889 associated with a shallow methane seep in the tropical Timor Sea of Australia reveals a novel aerobic
890 methanotroph diversity, *FEMS Microbiol. Ecol.*, 68, 142-151, 2009.

891 Wenner, P. G., Bell, P. G., van Amerom, F. H. W., Toler, S. K., Edkins, J. E., Hall, M. L., Koehn, K., Short,
892 R. T., and Byrne, R. H.: Environmental chemical mapping using an underwater mass spectrometer,
893 *Trac-Trend Anal. Chem.*, 23, 288-295, 2004.

894 Wiesenburg, D. A. and Guinasso, J. N. L.: Equilibrium solubilities of methane, carbon monoxide, and
895 hydrogen in water and sea water, *J. Chem. Eng. Data*, 24, 356-360, 1979.

896 Wunsch, C. and Ferrari, R.: Vertical mixing, energy, and the general circulation of the oceans, *Annu.*
897 *Rev. Fluid Mech.*, 36, 281-314, 2004.

898
899
900
901
902
903

904 Tables

905 Tab. 1 Classification of partial 16S rRNA gene sequences (Fig. 7) to bacterial taxa performed with the
906 Silva classifier (Pruesse et al., 2012). The confidence value (0–1) for assignment at the level of class
907 and genus is given in parentheses.

No.	Class	Family
1	Alphaproteobacteria (0.4)	<i>SAR11 clade</i> (0.2)
2	Cyanobacteria (1)	<i>Chloroplast</i> (1)
3	Alphaproteobacteria (1)	<i>Rhodobacteraceae</i> (1)
4	Bacteroidetes incertae sedis (0.43)	<i>Marinifilum</i> (0.4)
5	Alphaproteobacteria (1)	<i>Rhodobacteraceae</i> (1)
6	Alphaproteobacteria (1)	<i>Rhodobacteraceae</i> (1)
7	Alphaproteobacteria (1)	<i>Rhodobacteraceae</i> (1)
8	Cyanobacteria (1)	<i>Synechococcus</i> (1)
9	Cyanobacteria (1)	<i>Synechococcus</i> (1)
10	Gammaproteobacteria (1)	<i>Pseudoalteromonadaceae</i> (1)
11	Proteobacteria (0.36)	
12	Alphaproteobacteria (1)	<i>Rhodospirillaceae</i> (0.8)
13	Alphaproteobacteria (0.91)	<i>Rhodospirillaceae</i> (0.7)

908

909

910

911

912

913

914

915

916

917

918

919

920

921

922

923

924

925 Tab. 2 Comparison of highest methane concentrations, methane oxidation rates, and sea-air fluxes from different locations

Location	Methane concentration <i>up to nM</i>	MOx-rate <i>nM day⁻¹</i>	SAF <i>nmol m⁻² s⁻¹</i>	Reference
Seep sites				
central North Sea	1628	0.04-840	0.02-8.3	this study
Coal Oil Point, Santa Barbara Basin	1900	0.02-30	1.8	Mau et al., 2012; Pack et al., 2011
Tommeliten, North Sea	268		10.8*	Schneider von Deimling et al., 2011
west of Prins Karls Forland, Svalbard	524	up to 0.8		Gentz et al., 2013
Eel River Basin	300	0.002-0.8		Valentine et al., 2001
Deepwater Horizon event				
Gulf of Mexico	180000	up to 820		Valentine et al., 2010
Gulf of Mexico	1000000	up to 5900		Crespo-Medina et al., 2014
Overall areas				
Baltic Sea	38		0.008-0.2	Gülzow et al., 2013
Southern Bight of the North Sea	372	0.0002-0.3	0.07-7	Scranton and McShane (1991)
general European shelf estimate	21		0.11-0.24	Bange, 2006
Lakes				
floodplain lake in south-eastern Australia	50000		8.3-2700	Ford et al., 2002
polyhumic lake in southern Finland	150000	30-14400	0.5-695	Kankaala et al., 2007
the subtropical Lake Kinneret in Israel	450000			Eckert and Conrad, 2007
freshwater reservoirs in India	156000			Narvenkar et al., 2013

*direct transport via bubbles

926

927

928 Figures

929 Fig. 1: Location of the study area in the central North Sea. The main currents are shown following
930 Howarth (2001). The map was drawn using GeoMapApp with 40 m contours.

931

932 Fig. 2: Overview of gas flares mapped in January 2014 and CTD stations sampled in July 2013 (S12-
933 S21) and January 2014 (W2-W12). Flares cluster in 5 distinct areas (cluster 1-5) and reach to 6 m
934 from the sea surface (e.g. cluster 2 in upper right insert), which corresponds to the echosounder's
935 transducer depth. Hence, most likely the gas transport extends to the sea surface. Cluster 1
936 corresponds to the gas seep area investigated by Gentz (2013) (lower right insert).

937

938 Fig. 3: Depth profiles of potential temperature, salinity, density (sigma theta), and oxygen for all
939 stations in both summer and winter field programs.

940

941 Fig. 4: A-B Contour plots of the dissolved methane concentrations measured in the water column in
942 July 2013 and January 2014. The 6 km transect was divided into an eastern (positive numbers) and
943 western part (negative numbers) starting from the center station at 0 km. Note the different
944 methane concentration scales, which are necessary to properly display the different concentration
945 ranges. The black dots indicate the sampled water depths.

946

947 Fig. 5: Box plot of methane concentrations recorded by UWMS on 21.07.2013. The times on the right
948 side refer to the start and end times of the rectangular transects the UWMS was towed along in the
949 vicinity of flare cluster 1 (Fig. 2) at each water depth. Profiles obtained with UWMS are consistent
950 with discrete water sampling data.

951

952 Fig. 6: A-C Methane oxidation rates versus water depth measured with ³H-methane in July 2013 (A),
953 with ³H-methane in January 2014 (B), and using ¹⁴C-methane as tracer in July 2013 (C). D Time series
954 of water samples collected during both field programs and incubated with ³H-methane.

955

956 Fig. 7: DGGE profile of 16S rRNA gene fragments of samples from different depth and stations in the
957 central North Sea. Numbers on the lines indicate excised and successfully sequenced DGGE bands,
958 whose phylogenetic assignment is listed in Tab. 1.

959

960 Fig. 8: Methane oxidation rate versus methane concentration. A Michaelis Menten kinetics of Eq. 7
961 (MM-kinetics) using the parameters $v_{max}=1000 \text{ nM day}^{-1}$ and $K_m=800 \text{ nM}$ for curve MM-kinetics 1 and
962 $v_{max}=100 \text{ nM day}^{-1}$ and $K_m=12000 \text{ nM}$ for curve MM-kinetics 2. Together, both curves encompass the

963 range of the enzyme kinetics available. B Close up of the data for MOx-rates $< 20 \text{ nM day}^{-1}$ and MM-
964 kinetics 2 in that range and the linear regression of all data ($R^2=0.82$).

965

966 Fig. 9: Sketch of transport and loss terms estimated for the study area in $\text{nmol m}^{-2} \text{ s}^{-1}$.

967

968 Fig. 10: Model results over the course of a year. The mixed layer depth (D) shows the time period of
969 water column stratification from May until August. The mixed layer deepens during this time until
970 the entire water column is mixed again. During stratification, the water column is separated in
971 surface (B) and bottom water (C) whereas during the rest of the year the entire water column is well
972 mixed with methane concentrations shown in B. A displays the sea-air flux based on monthly mean
973 wind speed derived from the stations shown in Fig. 1. Model simulations including solely vertical
974 transport processes are shown as gray to black lines, which illustrate the range due to different D_v
975 values (see text). The model simulation based on methane oxidation in addition to vertical transport
976 is shown as a red line.

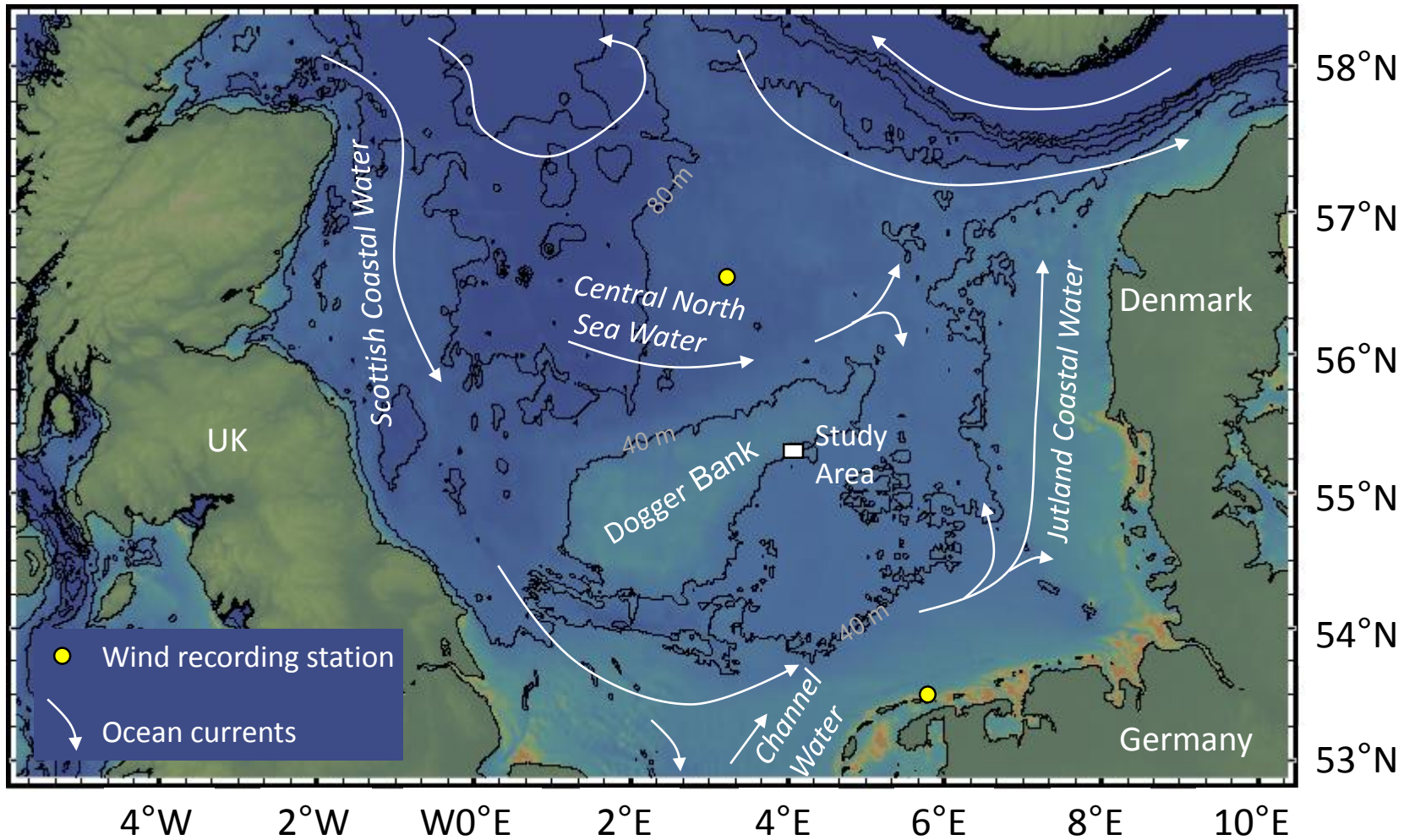


Fig. 1: Location of the study area in the central North Sea. The main currents are shown following Howarth (2001). The map was drawn using GeoMapApp with 40 m contours.

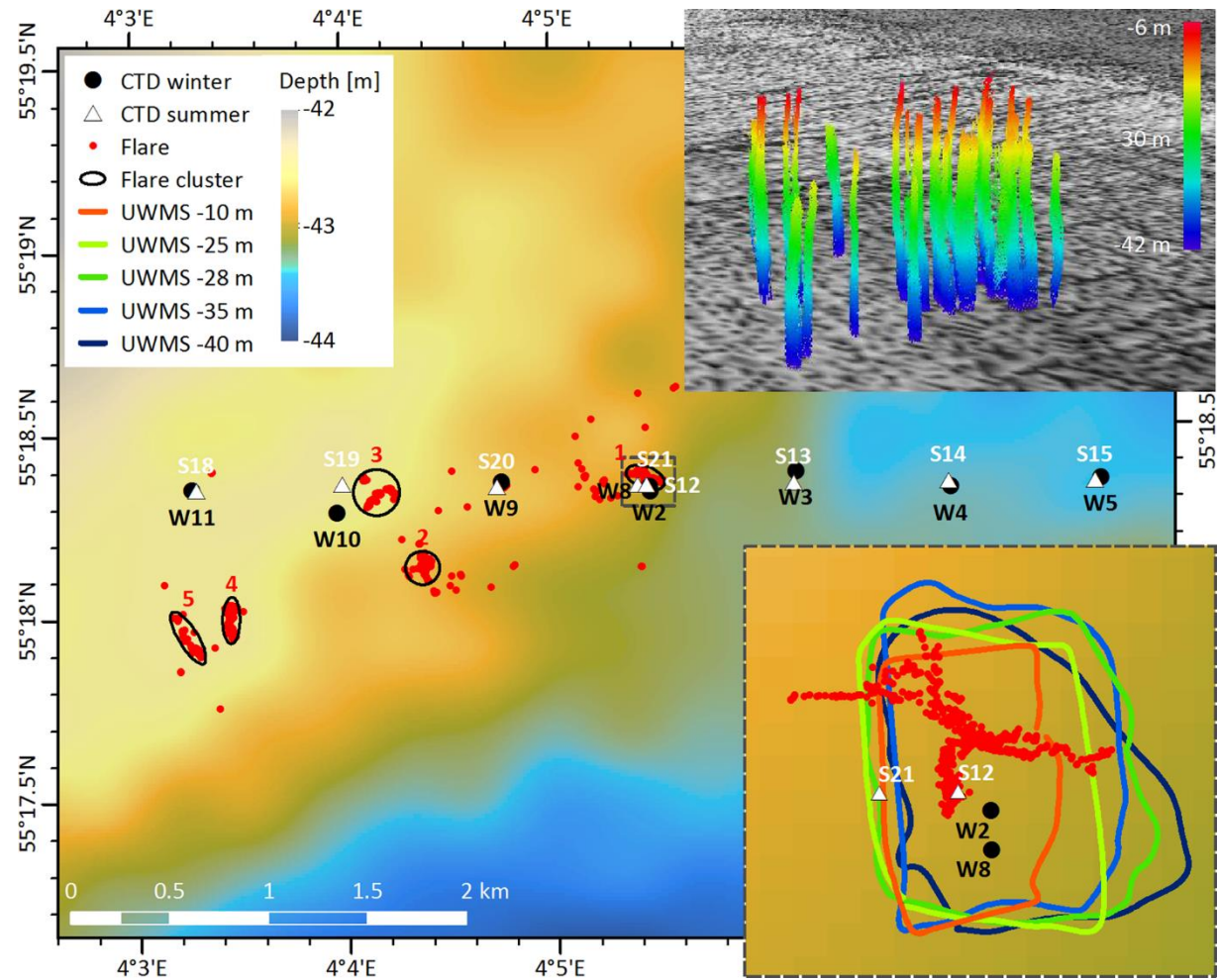


Fig. 2: Overview of gas flares mapped in January 2014 and CTD stations sampled in July 2013 (S12-S21) and January 2014 (W2-W12). Flares cluster in 5 distinct areas (cluster 1-5) and reach to 6 m from the sea surface (e.g. cluster 2 in upper right insert), which corresponds to the echosounder's transducer depth. Hence, most likely the gas transport extends to the sea surface. Cluster 1 corresponds to the gas seep area investigated by Gentz (2013) (lower right insert).

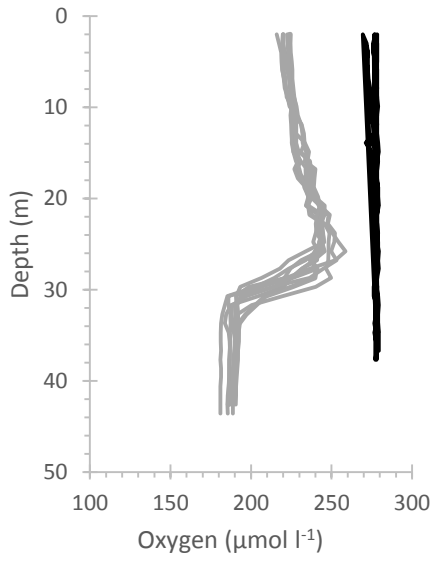
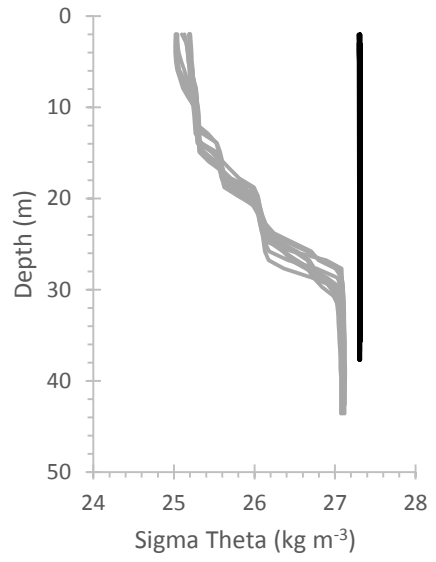
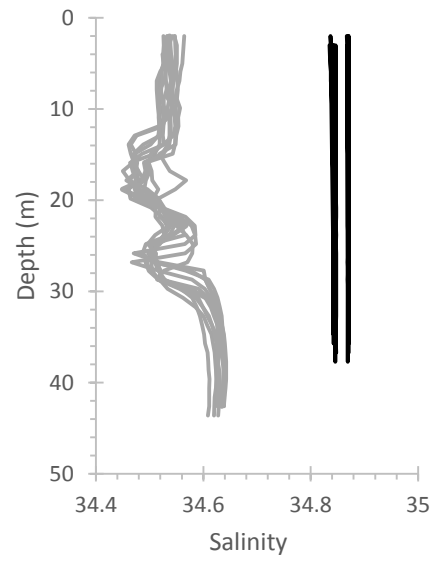
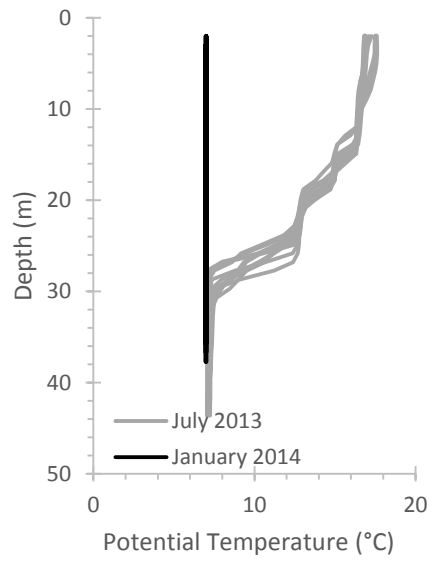


Fig. 3: Depth profiles of potential temperature, salinity, density (sigma theta), and oxygen for all stations in both summer and winter field programs.

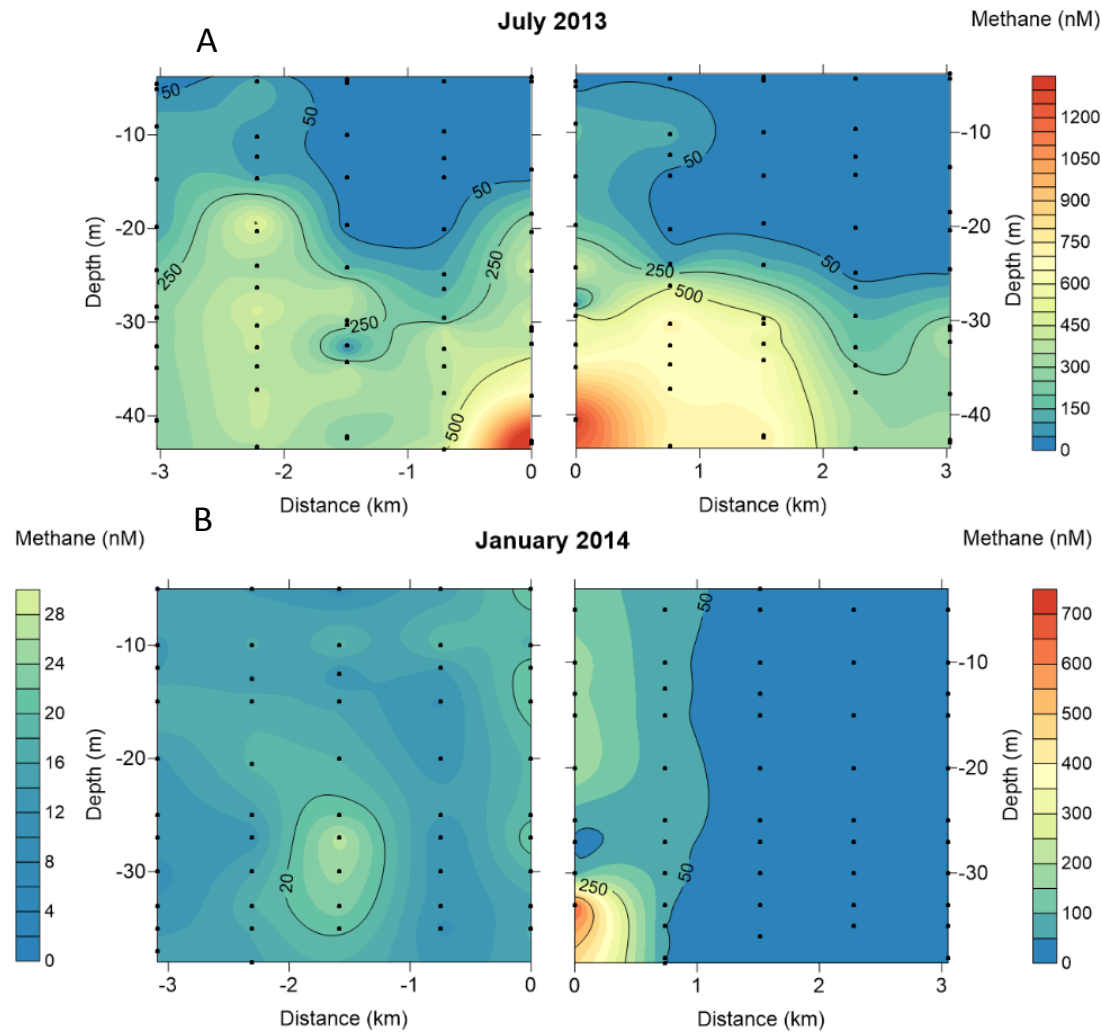


Fig. 4: A-B Contour plots of the dissolved methane concentrations measured in the water column in July 2013 and January 2014. The 6 km transect was divided into an eastern (positive numbers) and western part (negative numbers) starting from the center station at 0 km. Note the different methane concentration scales, which are necessary to properly display the different concentration ranges. The black dots indicate the sampled water depths.

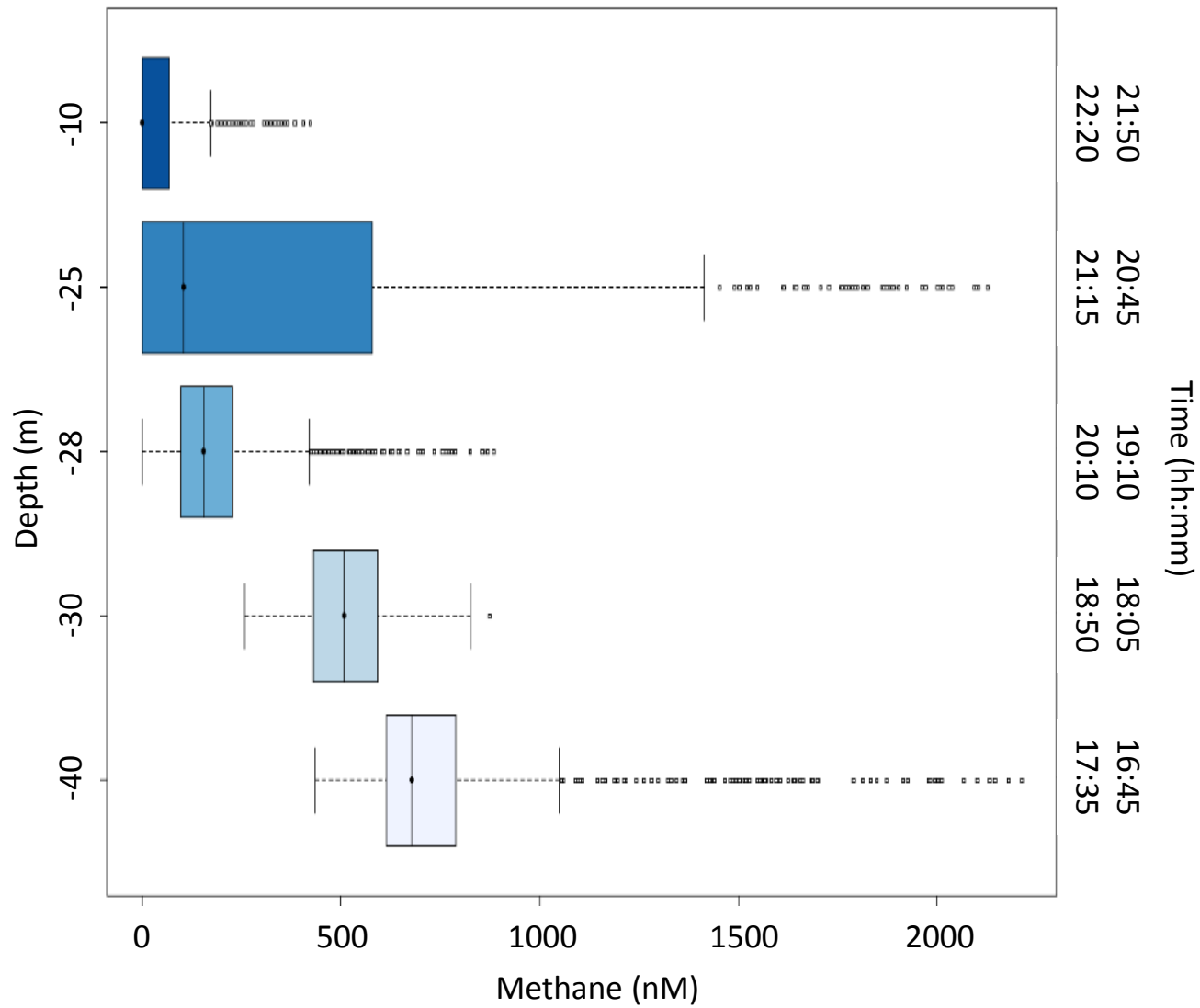


Fig. 5: Box plot of methane concentrations recorded by UWMS on 21.07.2013. The times on the right side refer to the start and end times of the rectangular transects the UWMS was towed along in the vicinity of flare cluster 1 (Fig. 2) at each water depth. Profiles obtained with UWMS are consistent with discrete water sampling data.

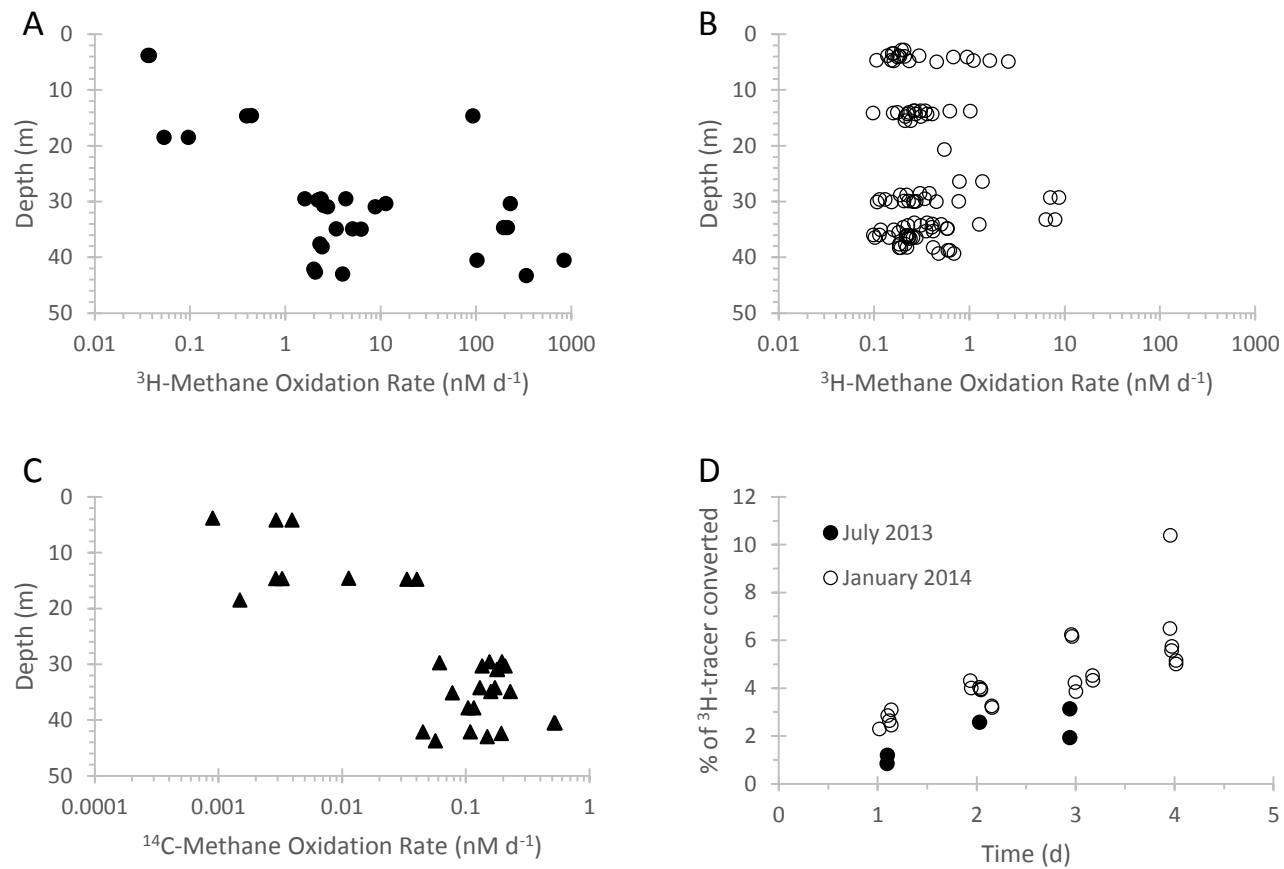


Fig. 6: A-C Methane oxidation rates versus water depth measured with ^3H -methane in July 2013 (A), with ^3H -methane in January 2014 (B), and using ^{14}C -methane as tracer in July 2013 (C). D Time series of water samples collected during both field programs and incubated with ^3H -methane.

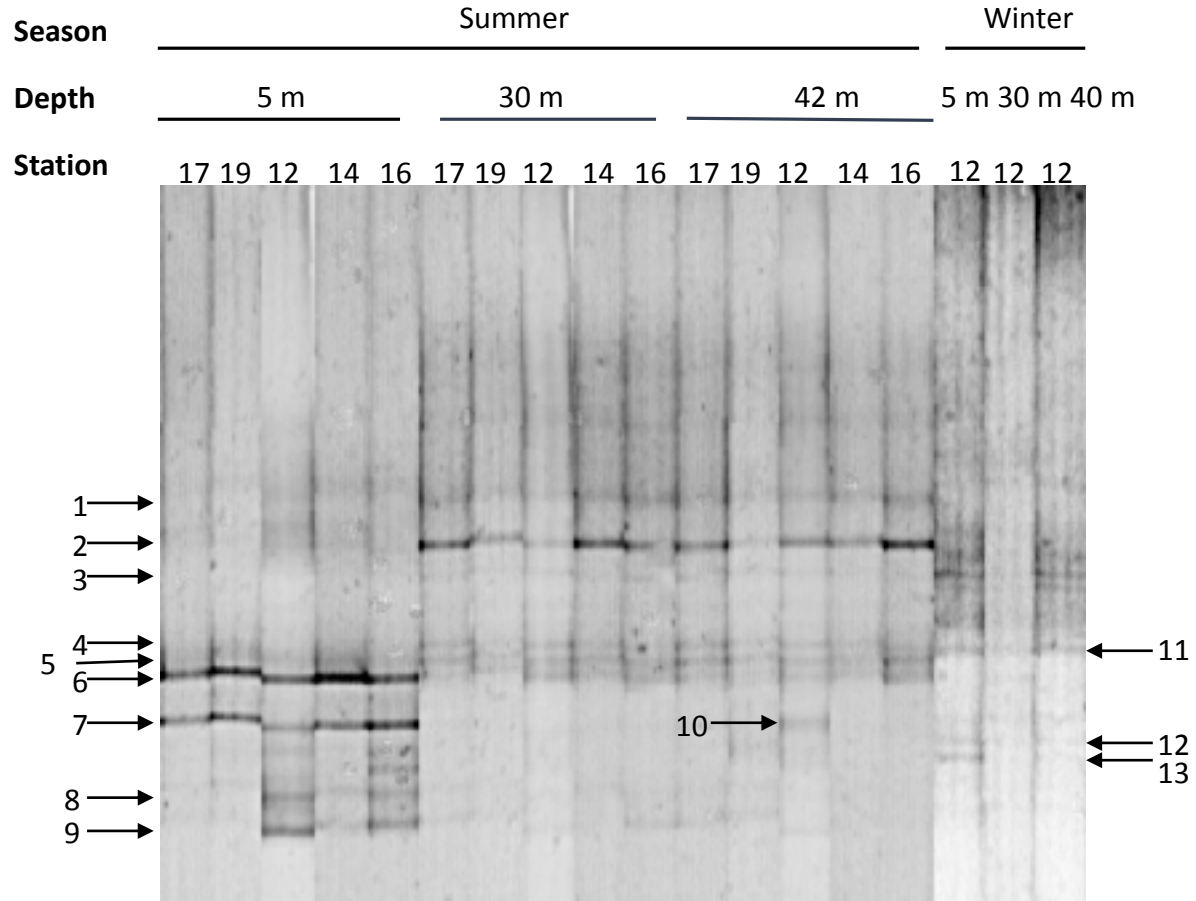


Fig. 7: DGGE profile of 16S rRNA gene fragments of samples from different depth and stations in the central North Sea. Numbers on the lines indicate excised and successfully sequenced DGGE bands, whose phylogenetic assignment is listed in Tab. 1.

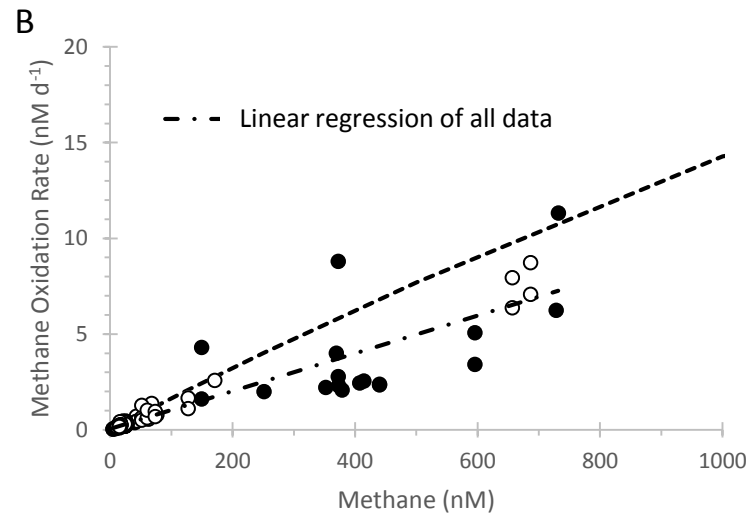
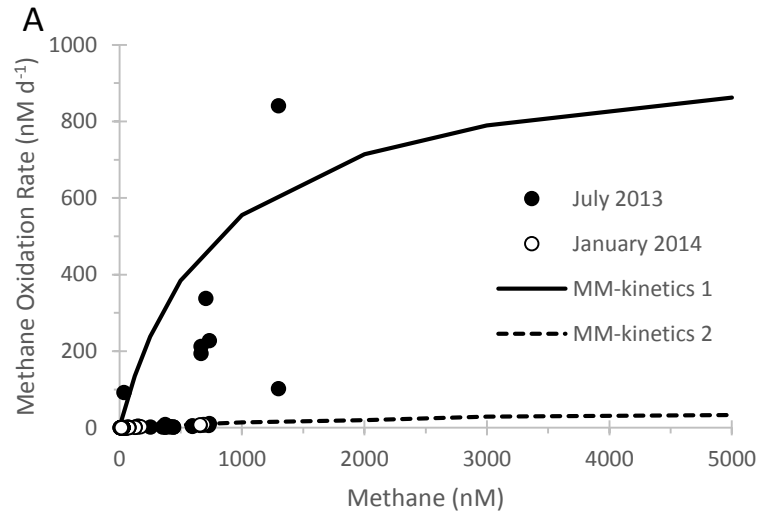
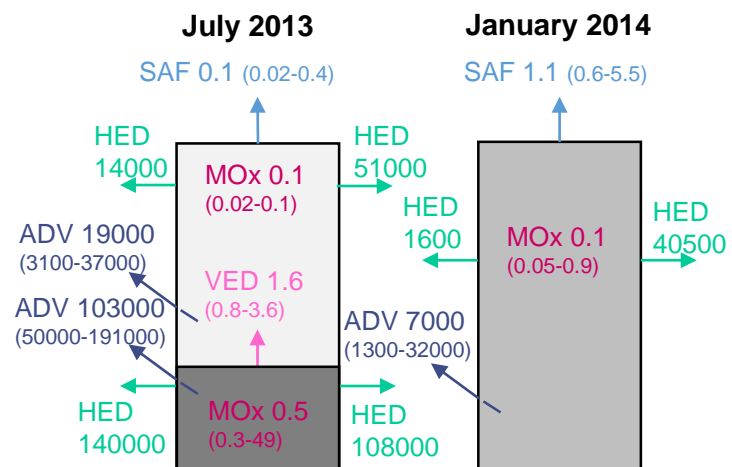


Fig. 8: Methane oxidation rate versus methane concentration. A Michaelis Menten kinetics of Eq. 7 (MM-kinetics) using the parameters $v_{max}=1000$ nM day⁻¹ and $K_m=800$ nM for curve MM-kinetics 1 and $v_{max}=100$ nM day⁻¹ and $K_m=12000$ nM for curve MM-kinetics 2. Together, both curves encompass the range of the enzyme kinetics available. B Close up of the data for MOx-rates < 20 nM day⁻¹ and MM-kinetics 2 in that range and the linear regression of all data ($R^2=0.82$).



SAF – Sea Air Flux
 MOx – Methane Oxidation rate
 VED – Vertical Eddy Diffusion
 HED – Horizontal Eddy Diffusion
 ADV – Advection
 Median of estimates (range of estimates)

Fig. 9: Sketch of transport and loss terms estimated for the study area in $\text{nmol m}^{-2} \text{s}^{-1}$.

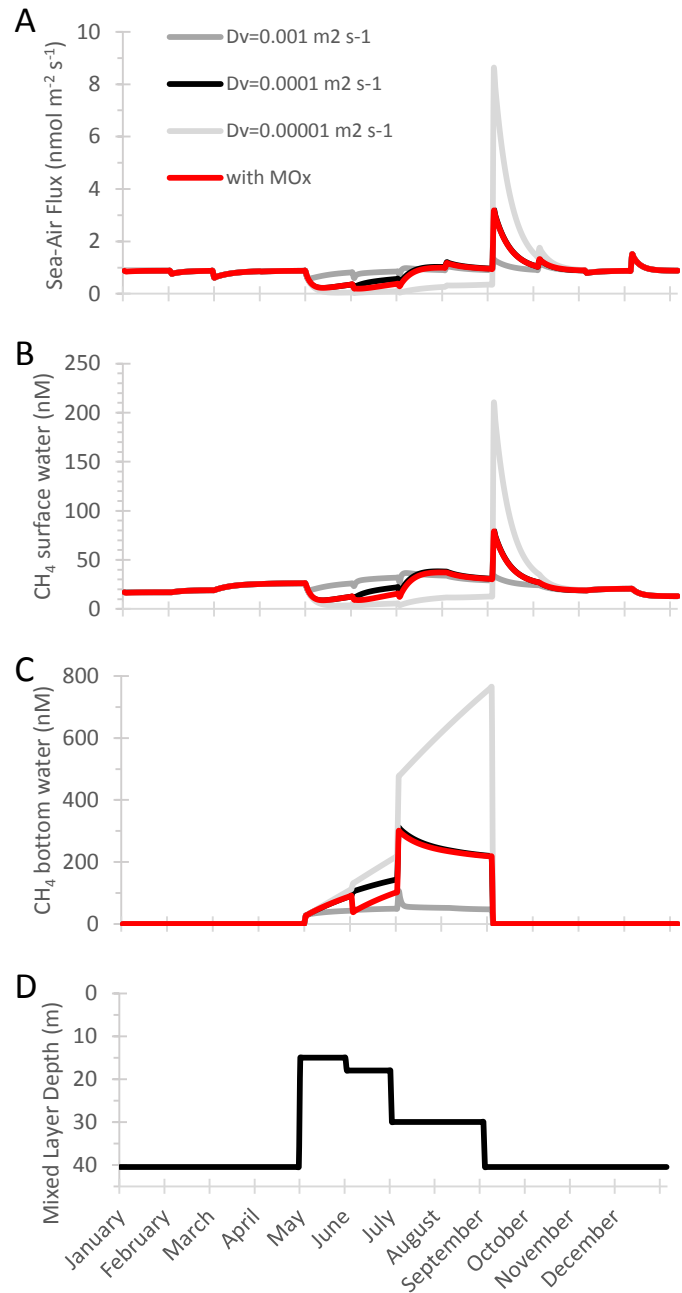


Fig. 10: Model results over the course of a year. The mixed layer depth (D) shows the time period of water column stratification from May until August. The mixed layer deepens during this time until the entire water column is mixed again. During stratification, the water column is separated in surface (B) and bottom water (C) whereas during the rest of the year the entire water column is well mixed with methane concentrations shown in B. A displays the sea-air flux based on monthly mean wind speed derived from the stations shown in Fig. 1. Model simulations including solely vertical transport processes are shown as gray to black lines, which illustrate the range due to different D_v values (see text). The model simulation based on methane oxidation in addition to vertical transport is shown as a red line.